J Neurophysiol 104: 2556–2572, 2010.
First published September 1, 2010; doi:10.1152/jn.01040.2009.

Trial-to-Trial Variability of Spike Response of V1 and Saccadic Response Time

Jungah Lee,[1] HyungGoo R. Kim,[2] and Choongkil Lee[1,2]
[1]*Department of Psychology,* [2]*Program of Brain Science, Seoul National University, Kwanak, Seoul, Korea*

Submitted 30 November 2009; accepted in final form 25 August 2010

Lee J, Kim HR, Lee C. Trial-to-trial variability of spike response of V1 and saccadic response time. *J Neurophysiol* 104: 2556–2572, 2010. First published September 1, 2010; doi:10.1152/jn.01040.2009. Single neurons in the primary visual cortex (V1) show variability in spike activity in response to an identical visual stimulus. In the current study, we examined the behavioral significance of the variability in spike activity of V1 neurons for visually guided saccades. We recorded single-cell activity from V1 of monkeys trained to detect and make saccades toward visual targets of varying contrast and analyzed trial-to-trial covariation between the onset time or firing rate of neural response and saccadic response time (RT). Neural latency (NL, the time of the first spike of neural response) was correlated with RT, whereas firing rate (FR) was not. When FR was computed with respect to target onset ignoring NL, a "false" correlation between FR and RT emerged. Multiple regression and partial correlation analyses on NL and FR for predictability of RT variability, as well as a simulation with artificial Poisson spike trains, supported the conclusion that the correlation between FR with respect to target onset and RT was mediated by a correlation between NL and RT, emphasizing the role of trial-to-trial variability of NL for extracting RT-related signals. We attempted to examine laminar differences in RT-related activity. Neurons recorded in the superficial layers tended to show a higher sensitivity to stimulus contrast and a lower correlation with RT compared with those in the lower layers, suggesting a sensory-to-motor transformation within V1 that follows the order of known anatomical connections. These results demonstrate that the trial-to-trial variability of neural response in V1 propagates to the stage of saccade execution, resulting in trial-to-trial variability of RT of a visually guided saccade.

INTRODUCTION

The activity of single neurons in the primary visual cortex (V1) shows a considerable variability in spike activity for repeated presentations of an identical visual stimulus (Schiller et al. 1976; Tolhurst et al. 1983; Vogels et al. 1989). Numerous studies have dealt with the source and functional significance of response variability. The variability of V1 activity may be explained by several factors, such as coherent fluctuations in membrane potential preceding the onset of a stimulus (Azouz and Gray 1999), on-going cortical activity reflecting the instantaneous state of cortical networks (Arieli et al. 1996; Kenet et al. 2003; Tsodyks et al. 1999), or stochastic properties of V1 neuron itself, such as intrinsic noise in thresholding for spike generation (Carandini 2004; Mainen and Sejnowski 1995; Schneidman et al. 1998; but see Fellous et al. 2004). Because spike trains of neurons in V1 are thought to relay stimulus information to motor areas responsible for visually guided behaviors such as saccadic eye movements, V1 seems to be a good place to test the role of spike variability for functional significance in visually guided behaviors. In this regard, a recent study examined the roles of V1 activity and found significant trial-to-trial covariation between V1 firing rate and behavioral choices of monkeys that were trained to detect a visual target of varying contrast that appeared in 50% of trials at a fixed position and to indicate target presence by making a saccadic eye movement toward it (Palmer et al. 2007).

Considering that there is a variation in spike time as well as firing rate (FR), an interesting question arises: does variability in neural latency (NL) or FR of V1 response correlate with behavioral latency as measured by saccadic response time (RT)? Neural correlates of RT variability have usually been sought beyond V1. For example, correlation with RT variability in visually guided saccade tasks was sought in neural activity in the frontal eye field (FEF) (Hanes and Schall 1996). It was found that RT variability was related to postperceptual motor activity but not to NL of FEF neurons (Thompson et al. 1996). In a related study on motion detection, RT was correlated with NL of the ventral intraparietal (VIP) areas but not with NL of the middle temporal (MT) area (Cook and Maunsell 2002). Thus it appears that NL and FR of cortical areas are variably related to RT.

Regarding covariation between NL of V1 and RT, two predictions can be contrasted. On one hand, trial-to-trial variability of NL, determined by the first spike time of response to visual target, may simply reflect noise fluctuating around the mean FR of V1 responses. Pooling spikes of V1 single neurons at downstream stages recovers FR by reducing this noise, and thus NL variability is uncorrelated with RT. Alternatively trial-to-trial variability of NL could be transmitted intact throughout subsequent processing stages up to saccade initiation, and NL may then vary with RT on a trial-to-trial basis. Thus the trial-to-trial variability in RT is inherited in part from V1 variability, and the origin of response variability can be traced from early sensory stages (Osborne et al. 2005). In the current study, we tested whether trial-to-trial variability of NL of V1 is correlated with that of RT in trained monkeys while they detected and made a saccade toward a stimulus appearing at one of multiple potential locations.

METHODS

Animal preparation

Two male Macaque monkeys (*IR,* a 6-yr-old Cynomolgous, and *CR,* a 5.5-yr-old Rhesus) participated in the current study. These monkeys were bred for research purposes and were housed in a dedicated colony for neurophysiology experiments. All experimental procedures were approved by the Seoul National University Animal

Address for reprint requests and other correspondence: C. Lee, Dept. of Psychology, Seoul National University, Seoul, Kwanak 151-742 Korea (E-mail: cklee@snu.ac.kr).

Care and Use Committee and conformed to the U.S. National Institutes of Health guidelines. No cataracts, retinal pathologies, or optic nerve head abnormalities in either monkey were observed with a slit lamp microscope and an indirect ophthalmoscope.

After several months of adaptation to the experimental environment, the animals underwent aseptic surgical procedures required for behavioral training and neural recording. They were first tranquilized with an injection of ketamine hydrochloride (5 mg/kg im; Yuhan), and given 0.1 mg im of atropine sulfate (Jeil Pharmaceutical). For prolonged anesthesia thereafter, sodium thiopental (Choongwae Pharmaceutical, 0.5 mg $\cdot$ $kg^{-1} \cdot h^{-1}$) was injected through an intravenous catheter placed in a vein of a hind leg. Body temperature was maintained around 37°C with a regulated heating pad. A scleral search coil made of three turns of 40 G multi-strand stainless-steel wire insulated with Teflon (Cooper Wire CA) with a diameter of 14–15 mm was implanted under the conjunctiva (Judge et al. 1980). The impedance of the coil was 70–90 Ω. For restraining the head, a cylindrical titanium post was mounted on the skull with the aid of a few custom-made titanium bolts whose thin heads were positioned underneath the skull, four to eight titanium bone screws, and bone cement containing an X-ray opaque synthetic resin (Palacos R, Biomet Merck Cementing Techonologies AB) mixed with antibiotic powder. The head post was positioned on the skull at AP −10 mm, ML 0 mm in a Horsley-Clarke stereotaxic frame (David Kopf Instruments). Custom-made titanium recording chambers (20 mm OD; height 10 mm) were implanted on the skull in the initial surgery, or in another surgery after 2–4 wk of behavioral training with the aid of the aforementioned bone cement. Two recording chambers were positioned as far posterior as possible but above the occipital ridge of the skull, in symmetric positions about the midline. At these positions, the major axis of each chamber was tilted posteriorly ~60°from the vertical, and the underlying V1 represented lower visual space. For the first 3 days of postoperative care, antibiotic ophthalmic ointment (terramycin, Pfizer) was applied to the eyes, antibiotic (cefazoline, 25 mg/kg, Jong Geun Dang) and antiinflammatory and analgesic (ketoprofen, 0.3 $ml \cdot kg^{-1} \cdot day^{-1}$, Uni Chemicals) injections were given.

One or 2 days before the first recording session, a craniotomy was performed. Under ketamine anesthesia, a small piece of skull (~4 mm diam) inside the recording chamber was removed, the dura exposed, and a small amount of antibiotic [mupirocin (Bactroban), Hanall] applied. The inside of the recording chamber was protected by a sterilized teflon cap tightly fit to the chamber. After the craniotomy, the dura was cleaned and thinned under light sedation (5 mg/kg ketamine hydrochloride) 5–17 h before each recording session, which greatly facilitated microelectrode penetrations. The thinning procedure typically took 10–20 min, and the animal started moving ~20 min after ketamine injection and was fully recovered from anesthesia by the time recording sessions started.

Animal training

After recovery from surgery, the animal was trained with its head restrained to make saccadic eye movements toward visual stimuli (Gabor patches) that were presented on a computer monitor. The target duration and contrast were systematically decreased from 300 to 50 ms, and from 90 to 0.5%, respectively, as the animal's performance improved. Correct movements were rewarded with a few drops of fruit juice delivered through a computer-controlled solenoid valve.

Eye positions were calibrated in two stages before each experiment using pursuit and fixation routines. A small image icon such as a banana or apple (0.38 × 0.38°) was used to determine the gain and offset of the eye position signal. It moved at a constant speed horizontally from −10 to +10° for 4 s, and vertically from −5 to +10° for 3 s. If the monkey's eye tracked the stimulus correctly, a juice reward was intermittently given. During horizontal tracking, the vertical offset was determined, and during vertical tracking the horizontal offset was determined. After tracking was completed, horizontal or vertical eye positions were displayed, and the gain of the monitoring system adjusted until the pursuit gain (horizontal or vertical pursuit velocity divided by target velocity) was unity. Then, the gain and offset were further adjusted with the fixation routine, in which the same stimulus was sequentially presented at predetermined locations along the horizontal (−10, −5, 0, 5, 10) and vertical (−5, 0, 5) meridians with intertrial intervals of 1s. The monkey was trained to follow the target for a juice reward that was delivered when the eye entered an electronically defined circular window with a radius of 0.5–2° around the target. Positions of the eye and target were displayed on a computer monitor, and when the eye and target position overlapped, a key was pressed to adjust the offset of calibration. The relationship between the voltage of the eye position signal and the angular gaze direction was assumed to be linear.

RT was determined in the following way. Signals related to horizontal and vertical eye positions were initially sampled at 25 kHz. These signals were down-sampled with a boxcar averaging with a window of 50 ms at 500 Hz and then differentiated to produce eye velocity vectors. Saccadic onset, i.e., RT, and offset were defined at the times when the eye velocity rose above and fell below the velocity of 15°/s, respectively. We compared RTs determined with boxcar, Chebyshev, and Gaussian filters in three example cells and found that there were no significant differences in RT distributions across filters. The boxcar filter was chosen for the analysis.

Experimental procedures

The animal was seated on a monkey chair, modified for recording stability from a commercially available model (Primate Products) with the head restrained and positioned at the center of magnetic field. The Teflon cap was removed from the recording chamber, and the inside of the chamber cleaned with sterile saline. In each recording session, extracellular single-unit activity was recorded from the primary visual cortex (V1) with one to three quartz-insulated platinum-tungsten microelectrodes (Thomas Recording). The microelectrodes were advanced with a five-channel minidrive (Thomas Recording). The nominal diameter of the electrode was 80 μm, including insulation. The electrode typically had an impedance of 1–4 MΩ at 1 kHz. The microdrive was equipped with one to three microelectrodes and fitted to the recording chamber. Then guide tubes were lowered through the craniotomy until they just contacted the dura. Melted agarose (Agarose LE, SeaMatrix, 1.5% in saline) was cooled to 37° and applied around the guide tubes to promote recording stability. The microdrive moved each electrode independently in steps of 1 μm.

The computer (Master) for stimulus presentation (Intel 3.0 GHz, memory: 2 GB) used two monitors, one for presenting stimuli and the other for controlling the experimental paradigm. The stimuli were presented on a gamma-corrected 24-in flat CRT monitor (Sony GDM-FW900, 800 × 600 pixel at a refresh rate of 100 Hz) by computer programs written in Matlab (The Mathworks) using Psychophysics Toolbox (Brainard 1997; Pelli 1997). Another computer (Slave) was used to store and display data. The Master instructed the Slave when to start A/D of signals related to the eye position, neural activity, experimental status generated by the Master and stimulus onset time provided by a photodiode facing the stimulus monitor. All these signals were digitized at the rate of 25 kHz with a resolution of 16 bit (National Instruments) with the aid of the DAQ Toolbox (the Mathworks). The Slave analyzed and displayed acquired data in real time. The Master also sampled eye position at a rate of 500 Hz for trial control. All timing information described in the following text was extracted from the data stored in the Slave.

Waveforms of spikes were extracted and sorted on-line based on spike duration and peak-to-peak amplitude to aid quantitative determination of receptive field (RF) properties such as position, size, preferred orientation, and spatial frequency. More rigorous sorting was performed off-line for quantitative characterization of single-unit activity. Although spikes were detected with consistent criteria, they

could be contaminated from sources such as animal movements or overlapped spikes from different cells. For the purpose of filtering these contaminations, all valid spikes were superimposed first, and then a subset that intersected the user-defined voltage-time window was selected. After filtering, the waveforms of valid spikes were classified as belong to one, two, or three cells with a spike sorting algorithm based on principal component analysis and *k*-mean clustering, and Euclidean distances between each cluster were used to assign each spike to a suitable cluster (Lewicki 1998).

Each monkey participated 3–4 day/wk for the main recording sessions over a period of ~4 mo. Two behavioral tasks were used in the current study: a fixation task and a visual detection task. In the fixation task, the animal was required to maintain its gaze within an electronically defined window of 1.5° in radius centered about the fixation target at the center of the display, and receptive field (RF) properties were quantitatively characterized in an effort to find the optimal stimulus for a given cell prior to a visual detection task. Based on previous studies showing that V1 cells have Gabor-like RFs (Jones and Palmer 1987), we used cosine moving gratings to determine the RF properties of each cell. For initial qualitative RF mapping, the moving grating confined within a circular zone varied along eight dimensions: horizontal and vertical positions, diameter, spatial frequency, phase, orientation, luminance, and contrast. By listening to spikes on an audio monitor, we could approximate the best position, orientation, and spatial frequency. Then for a quantitative determination of RF, a stationary cosine grating confined within a circular zone was used with a forward correlation method in which gratings with varying dimensions were randomly presented for 200 ms in 6–10 repetitions with a gap period of 400 ms between gratings. Trials with same stimulus dimensions were sorted, and the associated spike activity was aligned on stimulus onset. Plots of spike raster and spike density function were displayed during the experiment. Mean FR was calculated for response magnitude from the poststimulus time period of 50–200 ms. Based on the response magnitude, tuning curves were plotted and fitted with a difference-of-Gaussians model by the least root mean squared error (Roberts et al. 2005; Sceniak et al. 1999). The model captured the shape of tuning curves better than a single Gaussian model. From the fitted model, optimal values of tuning were obtained. This procedure was repeated to derive the optimal values of the following dimensions in this order: horizontal and vertical positions, orientation, spatial frequency, and size. This order was found empirically to be most efficient.

In the visual detection task, the monkey first fixated a visual target at the center of the display and then made a saccadic eye movement toward a stationary Gabor stimulus with the orientation preferred by the cell under study (Fig. 1). The target stimulus appeared in one of two potential locations. For some sessions of *monkey IR,* the number of potential target locations was four. A tone (50 ms beep) signaled the start of a trial. The contrast (%) of the Gabor target was defined as $(L_{max} - L_{min})/(L_{max} + L_{min}) \times 100$, where L is the luminance of a point on the screen. Thus contrast could vary between 0 and 100%; contrast of 2, 4, 16, and 64% were employed. In *monkey CR,* neural responses to the 2% contrast target were weak, and only 4, 16, and 64% contrast stimuli were used. The fixation and Gabor targets were displayed on a gray background with a mean luminance of 1.79 cd/m^2. The position and contrast of the Gabor target were shuffled in a given block so the animal had no prior anticipation.

Data analysis

Invalid trials were discarded for off-line analyses. These included trials with unsteady fixation due to drift or jitter, multiple saccades toward the target, no saccade, a saccade with latency <40 ms or >600 ms, or an incorrect saccade made toward positions other than the Gabor target. About 12% of trials (4,074 of 33,722 trials) were discarded at this stage. From remaining 29,648 trials, invalid trials were further discarded for the following reasons. The variability in eye position during target presentation undoubtedly caused a variable response magnitude. Thus we excluded trials in which the eye was

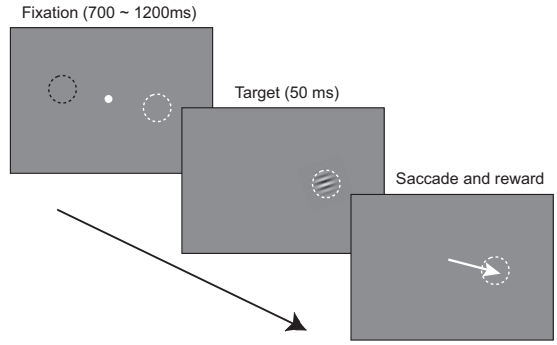

FIG. 1. Sequence of a trial. After a tone, the fixation target was presented at the center of the screen. The central fixation target was a red circle (0.2 × 0.2°, mean luminance 10.31cd/m^2), the edge of which was smoothed with a Gaussian filter. With a variable delay (700–1,200 ms) after the eye entered and remained within an electronically defined window around the fixation target, the fixation target went off and at the same time a Gabor target appeared for 50 ms at 1 of 2 or 4 locations. Dashed circles are only for illustration purposes and were not visible to the animal. The size of fixation window for selecting valid trials during off-line analysis was 1 × 1°. When 2 locations were used, 1 was the receptive field (RF) location (white dotted circle) and the other was directly across the fixation target as shown. When 4 locations were used, the 3rd and the 4th were along the directions perpendicular to the 1st 2. The animal's task was to detect the Gabor target and to make a saccade within 600 ms after target onset. When the animal failed to bring its gaze within a window of 4 × 4° around the target within 600 ms and maintain fixation for additional 500 ms, the trial was aborted. When the animals completed a trial successfully, they were given drops of fruit juice as a reward. The next trial started after an intertrial interval of 1 s.

deviated >3 SD from the mean fixation position. After excluding these trials, 99% of mean eye deviations were <0.5°, indicating that the fixation locations in virtually all valid trials remained within a 0.5 × 0.5° window during the target presentations. Also, trials with RT, mean FR, or NL >3 SD from the mean value of each parameter for each stimulus condition were excluded from further analyses. At this stage, 12% of trials (3,615 of 29,648 trials) were further discarded, and 26,033 trials were taken as valid and used for subsequent analyses. At least 20 valid trials were obtained for each condition of stimulus contrast and target position for each cell.

Most V1 neurons did not show a reliable response to targets with 2% contrast, so in some recording sessions the target with 2% contrast was not used. To quantify the magnitude of visual response, a modulation index was defined as (peak activity – baseline activity)/(peak activity + baseline activity), where peak activity is the maximal spike density during the poststimulus period of 0–200 ms, and baseline activity is the mean spike density during the period of 200 ms immediately preceding stimulus onset. A modulation index exceeding 0.3 was taken as indicating a reliable visual response and accepted for further analyses. This cutoff did not change the main results; no significant difference in Spearman simple correlation for NL or FR were found between with and without cutoff (260 contrast conditions from selected cells with modulation index > 0.3 vs. 295 conditions from all cells; 2 sample *t*-test, $P = 0.98$ for NL, $P = 0.97$ for FR50).

V1 activity can be measured in multiple ways, and different measures are thought to encode different aspects of the stimulus. For example, spike count or rate is related to the identity of the visual stimulus, whereas neural latency is related to stimulus contrast (Gawne et al. 1996b; Wiener and Richmond 1999). In the current study, the primary goal of the analysis was to relate measures of neural activity to saccadic latency. For this, we extracted two parameters: NL and FR.

Determination of NL

We defined NL as time from target onset to the time of the first spike of visual response, which in turn was defined from the spike density function as explained in the following text. Spike density

functions have traditionally been constructed to estimate the magnitude of spike activity by convolving the spike sequence with a Gaussian kernel function of a specific or variable SD (Richmond et al. 1990; Schall et al. 1995; Segraves and Park 1993) based on the assumption that a spike could have occurred at different times with the probability represented by the width of the Gaussian. However, this systematically underestimates neural latency by an amount depending on the width of the Gaussian function. To avoid this problem, the spike train was convolved with an asymmetric kernel function of the following equation (Thompson et al. 1996), $R(t) = (1 - e^{-t/\tau_g}) \cdot (e^{-t/\tau_d})$, where τ_g and t_d are time constants for the growth (1 ms) and decay (20 ms) phases, respectively. The following procedures were used to extract the first spike time from the spike density function. First, for each trial, the baseline discharge rate was calculated over the 200-ms interval immediately preceding stimulus onset. The distribution of baseline rate was compiled across all trials for a given cell, and the mean ± SD of the baseline rate was obtained. Then for each trial, the time of peak spike density was localized in the interval from target onset to saccadic onset, and time was searched backward from this peak until the value of the spike density function was ≤1 SD above the mean baseline discharge rate and remained at this level for ≥5 ms. NL was defined as the time of the first spike occurring after this threshold (Fig. 2). When various other values (100, 200, 300% of baseline rate) were used as threshold levels for a subset of 50 neurons included in this study, no significant differences in NL across threshold levels were found when the asymmetric kernel function was used (1-way ANOVA, $P = 0.32$), indicating the robustness of NL.

Because NL can be ambiguous in single trials due to the sparse and noisy nature of spike sequences of V1, we cross-confirmed NL with Poisson spike train analysis (Hanes and Schall 1996; Legendy and Salcman 1985; Maunsell and Gibson 1992; Sanger 2002; Schmolesky et al. 1998; Thompson et al. 1996; Xu et al. 1999). This method basically determines the time about which FR changes significantly as governed by a Poisson probability distribution (Hanes et al. 1995). This method has been used for the primary visual cortex in the awake monkey to determine the latency of neural response evoked by a high-contrast stimulus (Maunsell and Gibson 1992), and as one method for confirming the validity of NL, we determined the neural latency based on the Poisson spike train method, following the procedures described by Hanes et al. (1995). Although the Poisson spike train analysis is a useful and reliable technique in detecting bursting activity, it resulted in more invalid trials in which NL was not localized for V1 activity in response to low-contrast visual stimuli (2 or 4%), even with the significance level relaxed as for nonbursting activity (Hanes et al. 1995). The number of trials in which neural latency was well determined was less with the Poisson spike train method than with first spike time based on spike density: 456 versus 779, 3,568 versus 6,294, 5,626 versus 8,030, and 6,425 versus 8,228 trials, for 2, 4, 16, and 64% contrast, respectively, or 41, 43, 30, and 22% less with Poisson spike train method. This difference led us to opt for the first spike time based on spike density for estimating NL. However, the distributions of NL obtained with the first spike time based on spike density and Poisson spike train analysis did not differ significantly within each stimulus contrast or for the overall mean (mean NL determined with spike density was 64.77 ± 17.08 and that with Poisson distribution was 60.11 ± 21.83, 2-sample *t*-test, $P = 0.12$). The NL for the highest contrast (64%) ranged from 34.80 to 82.84 ms, consistent with Palmer et al. (2007), who reported that 36 ms was the shortest latency associated with the highest-contrast targets in their visual detection paradigm. Unless otherwise indicated, NL means "first spike time" calculated by the spike density function.

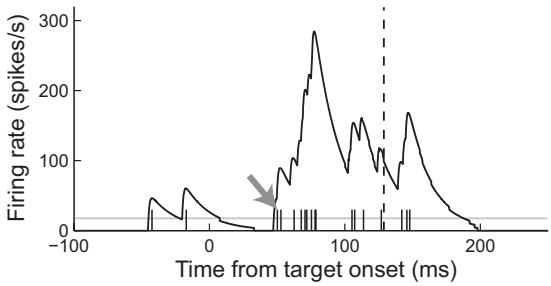

FIG. 2. Determination of neural latency (NL). *A*: spike density (black curves) was estimated by convolving the spike train (short vertical lines) with an asymmetric kernel function. Baseline spike rate was calculated for each trial over the prestimulus period of 200 ms, and the mean (gray horizontal line) ± SD of the baseline rate was determined for each cell. Then the time of peak spike density was localized in the interval from target onset to saccadic onset (vertical dotted line), and activity threshold was searched backward from this peak until the value of the spike density function was ≤1 SD above the mean baseline rate. The neural latency was defined as the time of the first spike (50.12 ms, gray arrow) occurring after this threshold. The spike sequence is taken from one of trials shown in Fig. 5*G*.

Difference in neural activity between earlier and later RT groups

Neural latencies derived with the preceding methods occasionally did not match those judged from visual impressions of spike trains. Therefore we tried to confirm the relationship between NL and RT by examining the difference in neural response between earlier and later RT groups. For each cell, trials for each stimulus contrast were divided into shorter and longer RT groups with respect to median RT. Spike density functions were derived separately for two RT groups, and the start times of visual response (1 SD over the baseline activity calculated over all trials) was compared between these two RT groups.

Determination of FR

To estimate FR for a given trial, the spike density was first derived by convolving the spike sequence with the above-mentioned asymmetric kernel function, and FR was estimated from the mean spike density. As will be shown in the following text, NL was correlated with RT, and thus to derive a measure of FR independent of NL, the mean spike density during the 50 ms immediately after NL was divided by this duration. We will refer to this FR as FR50 and use it as a measure of FR throughout the current paper. For another measure independent of NL, referred to as FR100, the FR of a trial was also derived from the mean spike density during an interval of 100 ms centered about the peak density divided by this duration.

Contrast sensitivity

Stimulus contrast is known to modulate the response and functional connectivity of V1 cells (Albrecht and Hamilton 1982; Nauhaus et al. 2009). Within the range of stimulus contrast used in the current study (2–64%), a logarithmic function provided an optimal description of the response (Fig. 3). As a measure of the sensitivity of each cell to change in stimulus contrast, we used the slope of contrast response function, *contrast sensitivity,* derived from a linear regression relating response magnitude to stimulus contrast, $r = Cs \times \log_{10}(\text{contrast}) + A$, where r is FR50, Cs is contrast sensitivity, and A is a constant reflecting a minimum discharge rate. Thus contrast sensitivity is the magnitude of change in FR50 per log unit increase of stimulus contrast, reflecting a sensory signal of neural activity.

Partial correlation analysis

Changes in neural activity related to stimulus contrast enabled the evaluation of the sensory component of neural activity but confounded the relationship between neural activity and RT because stimulus contrast is related to both neural activity and RT. The correlation between neural activity and RT was analyzed within each contrast condition. Also the magnitude of correlation between mea-

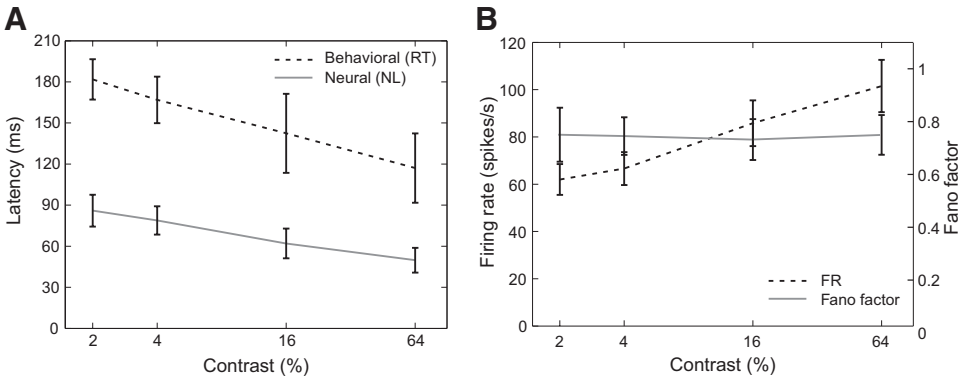

FIG. 3. Effects of stimulus contrast on NL and response time (RT, *A*) and FR50 and Fano factor of spike count (*B*). Each symbol represents the mean ± SD of the mean computed for each contrast for each cell from those trials in which saccades were made toward the Gabor target at RF. FR and FF were calculated over the temporal interval of 50 ms after NL. Note that data from 2 monkeys were combined except the condition of 2% contrast for which data were collected from only 1 monkey. See text for detail.

sures of neural activity and RT was estimated with a partial correlation coefficient for pooled data combined over all contrast conditions. The distributions of RT, NL, and FR50 were positively skewed; the mean skewedness of RT was 0.28 ± 0.74 and was significantly different from zero (1-sample *t*-test, $P < 0.01$), that of NL was 0.55 ±0.76 ($P < 0.01$), and that of FR50 was 0.39 ± 0.48 ($P < 0.01$) with no significant difference in skewedness across contrast (Kruskal-Wallis ANOVA test comparing skewedness, $P = 0.06$, 0.48, and 0.06 for RT, NL, and FR50, respectively). These results indicated that the distribution of each variable was contrast-independent and that data could be combined across contrast for further analysis. In the current study, all correlation and partial correlation coefficients were computed with the Spearman correlation, which makes no assumption regarding population distribution. Partial correlation analysis is aimed at finding a correlation between two variables while controlling for the contributions of confounding variables. In this study, partial correlation analysis was especially useful, as stimulus contrast is related to both RT and V1 activity (Fig. 3). Partial correlation coefficients were calculated between RT and NL and between RT and FR50.

Analysis of eye position

One potential source of the variability in spike response is variability in eye fixation during stimulus presentation from trial to trial (Gur and Snodderly 2006). To minimize fixation variability, we selected during off-line analysis the trials in which the eye position fell within a 0.5 × 0.5° window during target presentation as explained in the preceding text. However, the possibility remains that small variability in eye position at the time of stimulus presentation can influence the visual response of V1 neurons. To examine this possibility, we first performed a correlation analysis between eye movement parameters and V1 activity. The grand mean (±SD) of average eye velocity during the 50-ms target presentation across 101 cells was 0.86 ± 2.26°/s. The mean (±SD) Spearman correlation coefficient between the average eye velocity during the 50-ms target presentation and NL was 0.01 ± 0.18 and not significantly different from zero (1-sample *t*-test, $P = 0.19$), and that between eye velocity and mean FR50 was 0.01 ± 0.20 (1-sample *t*-test, $P = 0.25$). Similarly, the mean peak velocity of the eye during target presentation was 12.79 ± 7.89°/s, and it also showed near-zero correlation coefficients (0.02 ± 0.20, 1-sample *t*-test, $P = 0.05$ for NL; −0.00 ± 0.20, $P = 0.70$ for mean FR50). The effects of absolute distance between eye position and the fixation target during target presentation were also analyzed. The mean eye deviation was 0.27 ± 0.26°. The mean Spearman correlation coefficient between z-scores of eye deviation (eye deviation subtracted by the mean and divided by the SD) and NL was 0.01 ± 0.18 (1-sample *t*-test, $P = 0.32$) and that between *z*-scores of eye deviation and FR50 was −0.00 ± 0.21 (1-sample *t*-test, $P = 0.47$). These results indicate that eye movements during target presentation in our experimental condition were small and did not systematically influence V1 visual activity. We also examined the effects of phase deviation of the Gabor target caused by eye deviation from the center of the fixation target. When making a small eye movement, the phase of the stimulus would accordingly shift with respect to gaze line, inevitably resulting in a change in the activity of phase-sensitive neurons. Deviation of stimulus phase caused by gaze deviation from the center of fixation was determined from the horizontal and vertical eye positions during stimulus presentation and from the orientation and spatial frequency of the Gabor stimulus. If neural activity perfectly depends on stimulus phase, the relation between neural activity and the amount of eye deviation in the dimension orthogonal to the Gabor orientation within one cycle of spatial frequency of the Gabor stimulus would be sinusoidal. However, the sum of squared errors of linear and cosine fitting for relationship between above-mentioned phase deviation caused by eye deviation and FR50 or NL were not significantly different ($P = 0.86$ for NL, $P = 0.79$ for FR50). Neither the mean slopes of the linear fit were significantly different from zero (0.0 ± 0.1, 1-sample *t*-test, $P = 0.54$ for NL; 0.01 ± 0.10, $P = 0.13$ for FR50) nor were the mean slopes of the cosine fit statistically distinguishable from zero (0.19 ± 2.13, $P = 0.24$, for NL and 0.37 ± 2.10, $P = 0.99$, for FR50). These results indicate that potential phase deviations caused by small eye deviations after excluding outlying trials, although influencing the magnitude of neural activity did not influence neural responses in such a way that a significant correlation between NL and RT was artifactually produced. This is consistent with a previous study (Palmer et al. 2007) in which a similar analysis was performed.

Monte Carlo simulation for population analysis

The variability of single-cell activity may cause perceptual ambiguity and false alarm decisions and one way to avoid this is to pool spikes from the population of simultaneously active neurons (Shadlen and Newsome 1998). We evaluated the extent to which pooling single-cell activity increased information content regarding RT. First, we checked the correlation of neural activity between pairs of neurons simultaneously recorded with the same microelectrode. The mean Spearman correlation coefficients across 69 stimulus conditions for 25 pairs of well-isolated cells were 0.06 ± 0.20, 0.07 ± 0.13, and 0.08 ± 0.16 for NL and 0.10 ± 0.24, 0.02 ± 0.23, −0.04 ± 0.18 for FR50, for 4, 16, and 64% contrast conditions, respectively. These are rather small and vary in significance; coefficients for NL are significant ($P < 0.05$) in the 4 and 64% conditions and nonsignificant in the 16% conditions, and those for FR50 are nonsignificant in all contrast conditions. We conclude that the correlation of NL or FR50 between neuron pairs is negligible. These correlations are considerably lower than those previously reported for V1 (Gawne et al. 1996a; Kohn and Smith 2005) and for other parts of the brain (Bair et al. 2001; Gawne and Richmond 1993; Lee et al. 1998). A potential reason for this discrepancy is the shorter analysis window of the current study (Reich et al. 2001a) because the correlation coefficients for FR computed during a longer temporal window became significant for some stim-

ulus contrast; for example, the mean Spearman correlation coefficients for FR100 between the same pairs of neurons increased to 0.14 ± 0.25 ($P < 0.05$) from 0.10 ± 0.24 for 4% contrast condition. Due to saccade-related activity in V1 (Super et al. 2004) that may confound contrast-related change in FR correlation, extending analysis window from target onset was not practical. Also simultaneous spikes from neurons recorded with a single electrode, although they are uncommon, are difficult to isolate and tend to lower correlation (Bair et al. 2001). Note that the correlation for FR50 or FR100 is computed from spikes collected during temporal intervals different between paired neurons. The mean Spearman correlation coefficients for mean FR computed during 40–130 ms of poststimulus time period between the same pairs of neurons were 0.08 ± 0.25, 0.05 ± 0.28, and −0.02 ± 0.24, for 4, 16, and 64% contrast conditions, respectively, and nonsignificant in all contrast conditions.

At any rate, the near independence of the parameters used in the current study for neural responses between nearby neurons suggests that one can resolve response ambiguity by pooling these parameters across relatively few cells. To estimate the explanatory power of V1 populations for RT, we analyzed the performance of an ensemble of V1 neurons using a Monte Carlo simulation. *N,* ranging from 1 to 50, neurons were randomly selected from the pool of 66 of 101 recorded neurons that had ≥50 trials for each contrast condition. The trials for each contrast were sorted by associated RT into classes of 3 ms bin. The population activity of a trial was simulated by first randomly choosing stimulus contrast with a rectangular probability distribution and RT with a Gaussian probability distribution. Then the NL and FR were calculated from population spike trains combined from trials that were randomly chosen without replacement within the chosen stimulus contrast and RT class, one each from *N* single neurons. NL and FR of the simulated population spike train were calculated in the same way as for the single-cell data. Here we use FR during 40–130 ms of poststimulus time period instead of FR50 because FR50 sets different integration periods for pooled neurons due to variable NL, which would be physiologically unrealistic. This procedure was repeated for 300 simulated trials to calculate a partial correlation with RT. Partial correlations were calculated for 66 different pools of *N* neurons and the mean and SD of partial correlation were obtained. The partial correlation against population size was fitted with an exponential growth model, $y = \alpha - (\alpha - \beta)e^{-kx}$, where α is an upper asymptote, β is the initial value, and k is a scale parameter controlling the growth rate.

Simulation of the time course of correlation between FR and RT

As will be shown in the following text, trial-to-trial variability of FR50 was not correlated with RT, whereas FR computed for poststimulus time periods was. We performed a simulation study to gain insights regarding the conditions giving rise to this discrepancy. Poisson spike trains were generated in two conditions. In the first, FR of Poisson spike trains changed from a baseline level (10 spike/s) to a response level (100 spike/s) at a variable moment mimicking a variable NL and remained constant afterward throughout the trials. The variability of NL was randomly chosen from a Gaussian distribution with a mean of 60 ms, a sigma of 20, and a minimum of 35 ms. For simulating RT that is coupled to NL, saccadic onset time was generated with a delay from the NL, which was drawn from a Gaussian distribution with a mean delay of 150 ms, a sigma of 50 ms, and minimum delay of 80 ms. These numbers were close to those obtained experimentally (Fig. 3). In the second condition, the baseline FR changed at the same moment across trials to a variable response FR. The trial-to-trial FR variability followed a Gaussian distribution with a mean of 150, a sigma of 100, and a minimum of 5 spike/s. The variability was exaggerated for illustration purposes. To introduce a negative correlation between FR and RT, saccadic onset time was simply taken as minus FR plus a Gaussian random scatter. In both conditions, a random number drawn from a uniform distribution between 0 and 1 was compared with the instantaneous FR for generating a spike for each of sequential bins of 1 ms. Spike generation was prohibited within an absolute refractory period (3 ms), and this reduced the resultant FR of generated spike train slightly lower than the compared FR. In both conditions, Pearson correlation coefficients were computed between FR during sequential periods aligned at target onset and RT as done for experimental data.

RESULTS

Data summary

These results are based on 101 single cells sorted from extracellular action potentials recorded from 69 V1 sites in two monkeys (65 cells from *monkey IR,* 36 cells from *monkey CR*). The mean (±SD) eccentricity of RF center was 4.98 ± 1.49°, which was found optimal for reliable detection of saccadic eye movements. The mean spatial frequency was 1.23 ± 0.31 cycle/°, and the mean RF size (diameter of preferred Gabor target as determined by spatial summation method) was 2.80 ± 0.50°. Preferred orientations of the cells were fairly evenly distributed. The mean recording depth with respect to the first audible visual driving was 0.52 mm, ranging from 0 to 1.97 mm.

The detection performance of *monkey CR* was near chance for the stimulus contrast of 2%, and accordingly 2% contrast was not used for this monkey. Other than this, detection performance was excellent; the proportions of correct trials combined from the two monkeys were 83, 93.5, 95.5, and 96% for 2, 4, 16, and 64%, respectively, of stimulus contrast. As the stimulus contrast increased, NL systematically decreased and FR50 (FR during the period of 50 ms after NL, see METHODS) increased (Fig. 3). Also with the increase in stimulus contrast, RT decreased (Fig. 3*A*), consistent with previous studies (Carpenter 2004; Wheeless et al. 1966). The functions relating RT and NL to stimulus contrast were similar. The Fano factor (FF, variance/mean ratio) of spike count computed over the period of 50 ms after NL remained the same across stimulus contrast (0.75, 0.75, 0.73, and 0.75 for 2, 4, 16, and 64%, respectively). Similarly the variance/mean ratios of FR50 were 10.82, 11.16, 11.01, and 11.33 for 2, 4, 16, and 64% contrast conditions, respectively (not shown). No contrast pairs of FF of spike count or FR showed a significant difference across contrast. The FF of spike count found in the current study suggests that the stimulus was suboptimal (Gur and Snodderly 2006).

In Fig. 3, we combined data from the two animals to show an overall summary. The variables were mostly similar across contrasts between *monkeys IR* and *CR* in RT (144.44 ± 38.48 vs. 147.56 ± 16.01 ms, $P = 0.45$, Mann-Whitney U test for this and all subsequent tests), NL (65.58 ± 17.67 vs. 64.81 ± 14.84, $P = 0.66$), and mean FR50 (79.41 spike/s ± 47.60 vs. 90.49 ± 49.15, $P = 0.02$). Because *monkey CR* participated in only a two-target condition, two target conditions with 4, 16, and 64% contrast were used for these comparisons. For *monkey IR,* a four-target condition was also used. When the differences in RT, NL, and FR50 were compared between two- and four-target conditions in this animal using the nonparametric Mann-Whitney U test, RT and NL were larger and FR50 was lower in the two- than the four-target condition but not con-

sistently so in all conditions (Supplementary Table S1).[1] These results violate Hick's Law, which states that RT increases with the number of response alternatives. This violation has also been reported in previous studies using a visually guided saccade task similar to the one used in the current study (Kveraga et al. 2002; Lawrence et al. 2008) and appears to be mirrored in V1 activity. For *monkey IR,* 2% contrast was also used, and this counterbalanced the effects of four-target condition in this animal, resulting in the absence of overall differences in RT and NL. The differences between two- and four-target conditions noted from between-cell comparisons are ignored in Fig. 3, as the main focus of the current study was the relationship between RT and NL or FR analyzed within each stimulus condition for each cell.

The number of spikes during saccade latency increased with stimulus contrast. Overall the temporal interval from NL to RT decreased as contrast increased (95.85, 88.06, 80.48, and 67.28 ms for contrast conditions of 2, 4, 16, and 64%, respectively, Fig. 3*A*). The increase in FR50 with contrast overcompensated for the decrease in the interval, and the number of spikes observed during this interval from NL to RT increased with contrast; 3.94, 4.24, 5.93, and 6.25 spikes for 2, 4, 16, and 64% contrast, respectively. Similar estimates were obtained from normalized population spike density functions (Fig. 4); 4.40, 6.11, and 6.30 spikes for 4, 16, and 64% of stimulus contrast. Thus during the latent period of saccade, unequal number of spikes were generated.

Figure 4 illustrates the time course of population spike density averaged over 101 cells recorded in two monkeys for each stimulus contrast. With the increase in stimulus contrast, the onset time of firing increase was earlier, the rate of initial rise in FR was steeper, and the peak FR was higher.

Covariation between NL and RT

The covariation between NL and RT analyzed for each cell varied across sampled neurons. First, we show the activity of an example cell, and then we describe a quantitative summary of the covariation. Figure 5 illustrates spike activity of a single V1 cell that abruptly increased in response to a Gabor target appearing inside RF. If the cell activity reflects a sensory response to target appearance and if the variability of NL is not related to RT, the pattern formed by the marks of saccadic onset across trials sorted by NL (Fig. 5, *A, D,* and *G*) is expected to be vertical, i.e., unrelated to NL, as seen in similar plots for purely sensory cells in V1 (not shown). In other words, RT is expected to change depending on stimulus contrast but not by the variability of NL for purely visual cells. However, the fitted curve through saccadic onset marks is tilted following the variability of NL. Similarly the pattern formed by the marks of NL across trials sorted by RT (Fig. 5, *B, E,* and *H*) is not vertical but is tilted slightly following RT, which is not expected for purely sensory cells because the sensory response would be tightly coupled to target onset and unrelated to RT (DiCarlo and Maunsell 2005). There was a positive covariation between NL and RT within each contrast condition (Fig. 5, *C, F,* and *I*).

Figure 6 summarizes correlation coefficients between RT and NL for 101 cells recorded in two monkeys. The distributions of Spearman simple correlation coefficients (Fig. 6, *A–C*) indicate that NL and RT were correlated within each contrast condition. To combine results from correlation analysis performed within each contrast, we calculated the partial correlation between NL and RT controlling stimulus contrast. The average partial correlation between NL and RT controlling stimulus contrast was 0.23 ± 0.14 (1-sample *t*-test, $P < 0.01$, Fig. 6*D*).

Like mean NL and mean FR were inversely related with each other with respect to stimulus contrast (Figs. 3 and 4), the trial-to-trial variabilities of NL and FR were significantly correlated with each other; Spearman correlation coefficient between NL and FR50 was −0.15 ±0.14 ($P < 0.01$; Fig. S1) and that between NL and FR100 was −0.19 ± 0.23 ($P < 0.01$). Thus the correlation between NL and RT might be confounded by the effects of FR. However, partial correlation analyses indicated otherwise. Spearman partial correlation coefficients between NL and RT after controlling FR50 were 0.17 ± 0.16 ($P < 0.01$), 0.15 ± 0.15 ($P < 0.01$), and 0.18 ± 0.18 ($P < 0.01$) for 4, 16, and 64% contrast conditions, respectively. Similar significant correlations were obtained between NL and RT controlling FR100 (0.17 ± 0.17, $P < 0.01$ for 4%; 0.17 ± 0.16, $P < 0.01$ for 16%; 0.19 ± 0.17, $P < 0.01$ for 64%). These results show that that the decrease in the magnitude of correlation between NL and RT by controlling FR was small and indicate that the correlation between NL and RT was not mediated by FR.

Neural latency can be ambiguous in single trials. To deal with this, we used Poisson spike train analysis as another way of determining NL and cross-checked the results. For 2% contrast tested in one monkey, the Poisson spike train analysis (*monkey IR*) failed to determine the neural latency in a large number of trials. For 4, 16, and 64% contrast, the mean partial correlation between NL estimated with Poisson spike train analysis and RT was 0.25 ± 0.17 (1-sample *t*-test, $P < 0.01$). Distributions of partial correlation coefficient based on neural latency estimated with spike density functions and Poisson spike train analysis were not significantly different (0.23 ± 0.14 vs. 0.25 ± 0.17, 2-sample *t*-test, $P = 0.41$). The results

[1] The online version of this article contains supplemental data.

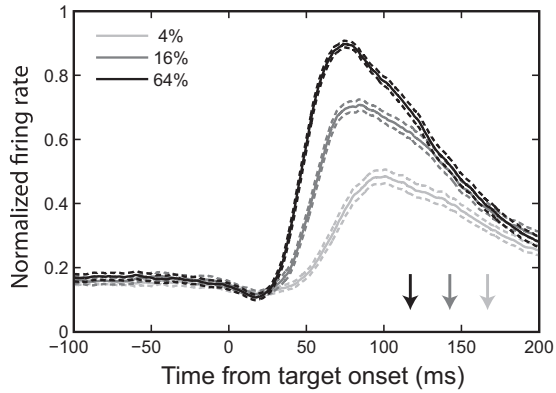

FIG. 4. Mean spike density function for each stimulus contrast averaged over 101 cells from 2 monkeys. The average spike density for each contrast for each cell was normalized by dividing maximum density across all contrasts of the cell and then averaged for all cells for each contrast. Note a consistent effect of stimulus contrast on the onset time of firing increase, the rate of initial rise in FR, and the level and timing of the peak FR. The dotted lines indicate SE, and arrows are mean RT for each contrast condition (166.86, 142.46, and 117.07 ms, for 4, 16, and 64%, respectively).

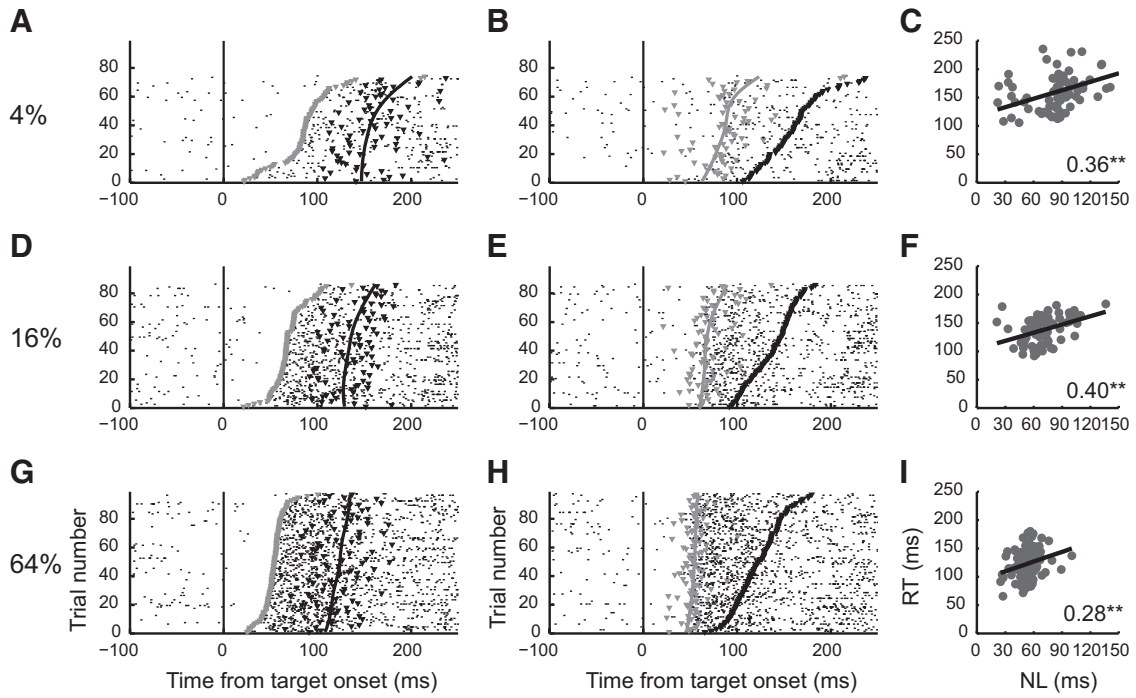

FIG. 5. Spike responses of a single cell recorded from V1 during valid trials in which the animal made successful saccades toward a Gabor target at RF of varying contrast of 4 (up), 16 (middle), and 64% (low). For each trial, the spike sequence is shown along with marks indicating NL (1st spike time, gray) and RT (saccade onset time, black marks). *A, D,* and *G*: trials are sorted according to NL, and spline approximations (black) are drawn through RT. *B, E,* and *H*: trials are sorted according to RT, and spline approximations (gray) are drawn through NL. *C, F,* and *I*: scatter plots of RT against NL and linear regression lines for 3 stimulus contrast conditions. Spearman correlation coefficients within contrast were significant (double asterisk, $P < 0.01$). These data demonstrate that for this cell, NL was correlated with RT for all contrast conditions. The trials in which the target was presented outside the RF across fixation are not shown. In these trials, spike activity was unaffected by either target or saccade. The cell's RF, and thus the Gabor stimulus used was at 6.2° in the right visual field and 1.6° down, with a diameter of 3°, a preferred orientation of 140 deg clockwise from 12 o'clock, and a preferred spatial frequency of 1.3 cycle/°. The cell was recorded 113 μm below the 1st audible sound of neural activity in a perpendicular penetration of dura and had a baseline activity level of 9.35 spike/s, a contrast sensitivity of 31.33, and Spearman partial correlation coefficient of 0.36 ($P < 0.01$) between NL and RT controlling stimulus contrast.

from both methods indicated that NL and RT varied together on a trial-to-trial basis.

We also examined the relationship between the onset of V1 response and RT in another way that does not depend on determination of NL by comparing the time course of spike response between shorter and longer RT groups. Trials within each stimulus contrast for each cell were sorted by RT and divided into shorter and longer RT groups about the median RT. If spike activity is unrelated to RT, the population spike activity would show no difference between the two RT groups. The onset of spike response of shorter RT group preceded that of longer RT group for all contrasts (1-sample *t*-test, $P < 0.01$, Fig. 7), again indicating that NL was related to RT. There were no significant differences

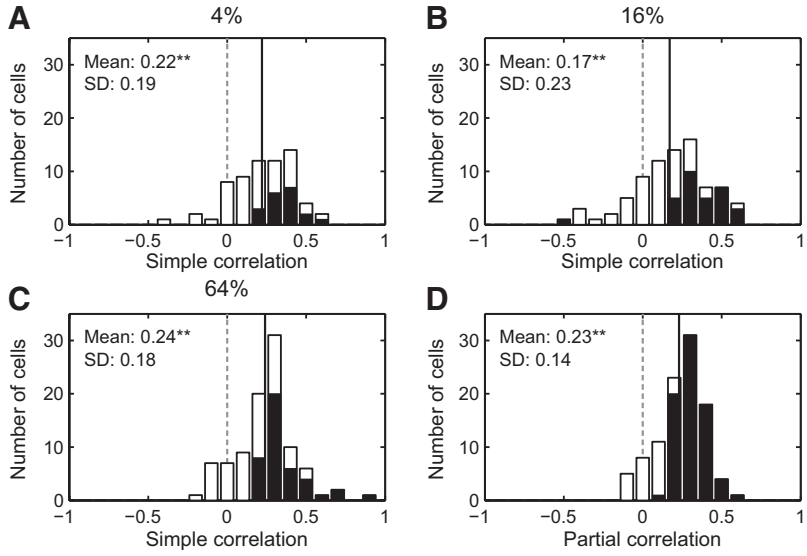

FIG. 6. Histograms of Spearman correlation coefficients between RT and NL. *A–C*: Spearman simple correlation coefficients for 101 cells for 2 monkeys for each stimulus contrast. *D*: Spearman partial correlation coefficients controlling stimulus contrast. ■, cells with significaint correlation coefficients ($P < 0.05$); —, the mean of distribution. Note that NL and RT are significantly correlated within each contrast condition.

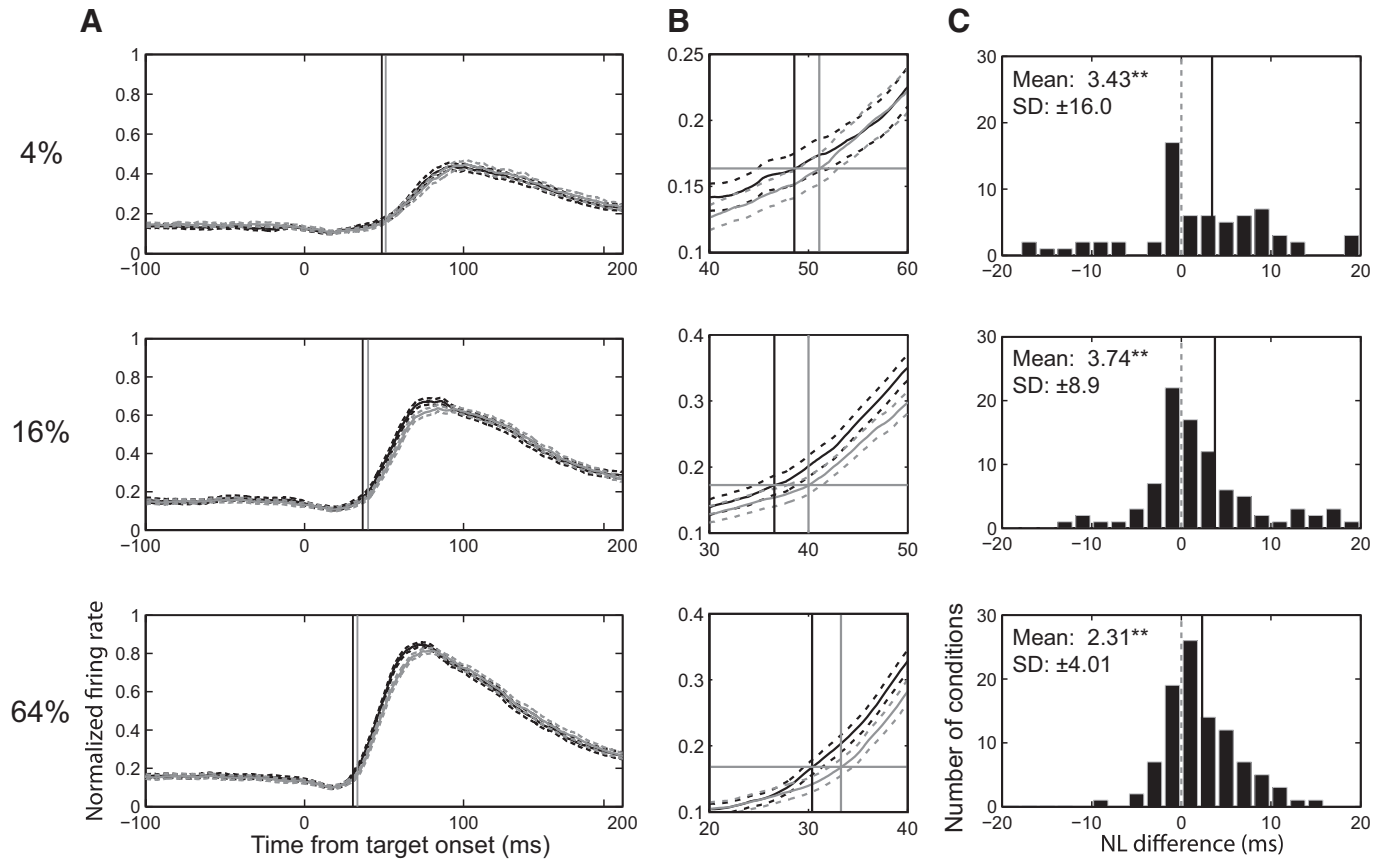

FIG. 7. Differences in neural response between 2 RT groups. *A*: population spike density functions combined from all 101 neurons for shorter (black) and longer (gray) RT groups for each contrast condition. For this, spike density for each cell was normalized such that the peak density was assigned 1. Curves are mean density and dotted curves are SE. *B*: magnified view of NL difference between the 2 RT groups of *A*. The population NLs of the 2 RT groups were determined by the criterion of 1 SD above a common overall baseline density (gray horizontal lines); black vertical lines for NL of the earlier RT group and gray vertical lines for NL of the later RT group (also shown in *A*). The differences in NL are 2.52, 3.44, and 2.92 ms for 4, 16, and 64% contrast conditions, respectively. *C*: histograms of difference of NL between the 2 RT groups. Solid vertical lines mark mean values. The NL difference was calculated by subtracting mean NL of shorter RT group from that of the longer RT group, and thus a positive difference indicates earlier timing in the shorter RT group.

between two monkeys in terms of difference between two RT groups; RT difference between the two RT groups was 27.93 ± 30.92 for *IR* and 28.38 ± 6.25 for *CR* ($P = 0.88$, 2-sample *t*-test between 2 animals), and NL difference between the two RT groups was 5.33 ± 19.19 for *IR* and 3.31 ± 17.36 for *CR* ($P = 0.37$).

Covariation between FR and saccadic response

We next determined the correlation between FR and RT. The correlation between FR50 and RT was distributed about zero (Fig. 8). Similarly, the average Spearman simple correlation between FR100 and RT was 0.02 ± 0.19, 0.01 ± 0.16, and 0.02 ± 0.19 for 4, 16, and 64% contrast conditions, respectively, and the average partial correlation between FR100 and RT controlling contrast was −0.01 ± 0.17; all these correlations were statistically nonsignificant. Therefore we conclude that trial-to-trial variability of FR was not correlated with RT.

We also determined if FR is related to saccade parameters other than saccade onset time, such as accuracy or amplitude. Saccadic accuracy was calculated from the distance between the eye position at the end of primary saccade and the target, and the mean and maximum velocity (either raw or rectified velocity) and vectorial amplitude of the primary saccade were calculated. Each of these measures were then correlated with each of various measures of FR, such as FR during 40–130 ms of poststimulus time period, FR during the period of 100 ms from NL, maximum FR, and FR during the period from NL to saccadic onset. Among resulting correlations, only the saccade amplitude and maximum saccade velocity for a stimulus contrast of 64% were significantly correlated with various measures of FR, and the mean rectified eye velocity was significantly correlated with maximum FR for 64% contrast condition. However, these correlations were all <0.08, and significant correlations were not found in other cases. Therefore we conclude that correlations between V1 activity and saccade amplitude and velocity are negligible.

The relationship between V1 neural activity and RT does not appear to be a byproduct of training or to be related to the spontaneous activity level of the cell. When total recording sessions in each monkey were divided into earlier and later halves, and partial correlations calculated for each, no significant differences in partial correlation coefficient were observed between the two halves in both monkeys. Overall, mean partial correlations between NL and RT were 0.24 ± 0.17 and 0.20 ± 0.11 for earlier and later halves, respectively, and this difference was not significant (Mann-Whitney *U* test, $P =$

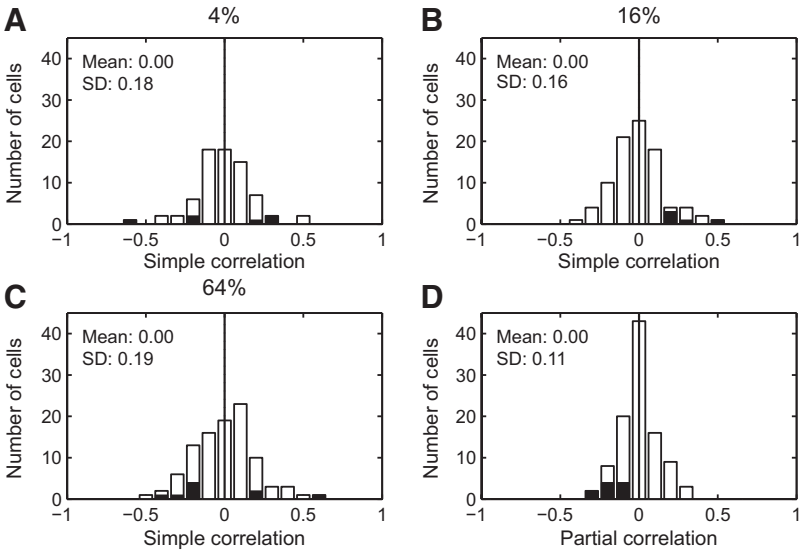

FIG. 8. Correlation between FR and RT. *A–C*: histograms of Spearman simple correlation coefficient between FR50 and RT for 101 cells from 2 monkeys. *D*: Spearman partial correlation coefficients between FR50 and RT controlling stimulus contrast. Same format as Fig. 6.

0.07). Mean partial correlations between FR50 and RT were -0.02 ± 0.14 and -0.00 ± 0.10 for earlier and later halves, respectively, and the difference was not significant either (Mann-Whitney *U* test, $P = 0.28$). The partial correlation was not related to the level of baseline (spontaneous) activity; the Spearman correlation between the mean baseline activity level of each neuron and partial correlation between FR50 and RT was -0.10 ± 0.25 ($P = 0.33$), and that for NL of the corresponding cell was 0.12 ± 0.36 ($P = 0.24$). No significant differences between the two monkeys were found for any of these analyses, and data from two monkeys were combined (Figs. 6–8). Specifically, the partial correlation coefficients between FR50 and RT were 0.00 ± 0.13 for *IR* and 0.00 ± 0.07 for *CR* ($P = 0.72$, Mann-Whitney *U* test for this and subsequent differences). The partial correlation coefficients between NL and RT were 0.24 ± 0.17 for *IR* and 0.23 ± 0.10 for *CR* ($P = 0.55$). When neural latency was estimated with the Poisson spike train method, the coefficients were 0.26 ± 0.20 for *IR* and 0.24 ± 0.12 for *CR* ($P = 0.24$).

Figure 9 illustrates time course of the correlation between FR and RT *with respect to target onset*. For this, a partial correlation between mean spike density and RT controlling stimulus contrast was calculated for each cell, separately for sequential 10-ms epochs spanning the 200 ms following target onset. The mean partial correlation of each epoch was calculated over all cells. A significant partial correlation between FR and RT emerged at 45 ms, peaked at 65 ms (maximal coefficient: -0.1 ± 0.02, 1-sample *t*-test, $P < 0.01$), and lasted for ~90 ms (40–130 ms marked with 2 vertical lines of Fig. 9). The range of epochs showing significant partial correlation between RT and FR was the same for both monkeys. Interestingly, the time of peak correlation was roughly the same as NL, and the time of peak correlation preceded the peak FR (compare Figs. 4 and 9), indicating that the time near the first spike carried the largest magnitude of correlation with RT and that the signal related to saccadic RT is extracted in a form separate from FR.

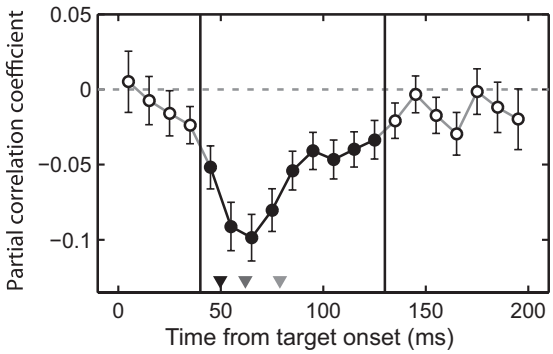

FIG. 9. Time course of correlation between FR and RT. Each symbol represents mean (with SE) of Spearman partial correlation coefficient for nonoverlapping poststimulus epochs of 10 ms between mean spike density and RT controlling stimulus contrast averaged over 101 cells. Filled circles, epochs of partial correlation significantly larger than 0 (1-sample *t*-test, $P < 0.01$). Triangles, mean NL for each stimulus contrast, 49.79, 61.98, and 78.80 ms for 64, 16 and 4% of stimulus contrast, respectively.

Simulation of "false" correlation between FR and RT

While trial-to-trial variability of FR50 (or FR100) did not show significant correlation with RT (Fig. 8), FR computed during the periods aligned on target onset did (Fig. 9). This apparent discrepancy could be due to covariation between NL and RT that artifactually produced false correlation between FR and RT when spike sequences of a variable NL were submitted to analysis windows fixed with respect to target onset. To understand the conditions giving rise to the time course of correlation between FR and RT of Fig. 9, we carried out a simulation study with Poisson spike trains generated in two conditions: a constant FR with a variable NL and a variable FR with a constant NL. Figure 10, *A* and *B*, shows artificial spike sequences and saccadic onsets generated in two conditions. Note that in the first condition, the FR of simulated trials was kept constant (100 spike/s) throughout the trial after NL and was not correlated with RT. However, when FR was computed during sequential periods aligned at target onset and correlated with RT, as done for experimental data, an artifactual correlation between FR and RT emerged, and the time course of correlation of Fig. 9 was closely mimicked (Fig. 10*C*). On the other hand, in the second condition in which RT was coupled to FR, the correlation between FR and RT, not surprisingly, changed after FR changed, and the time course of

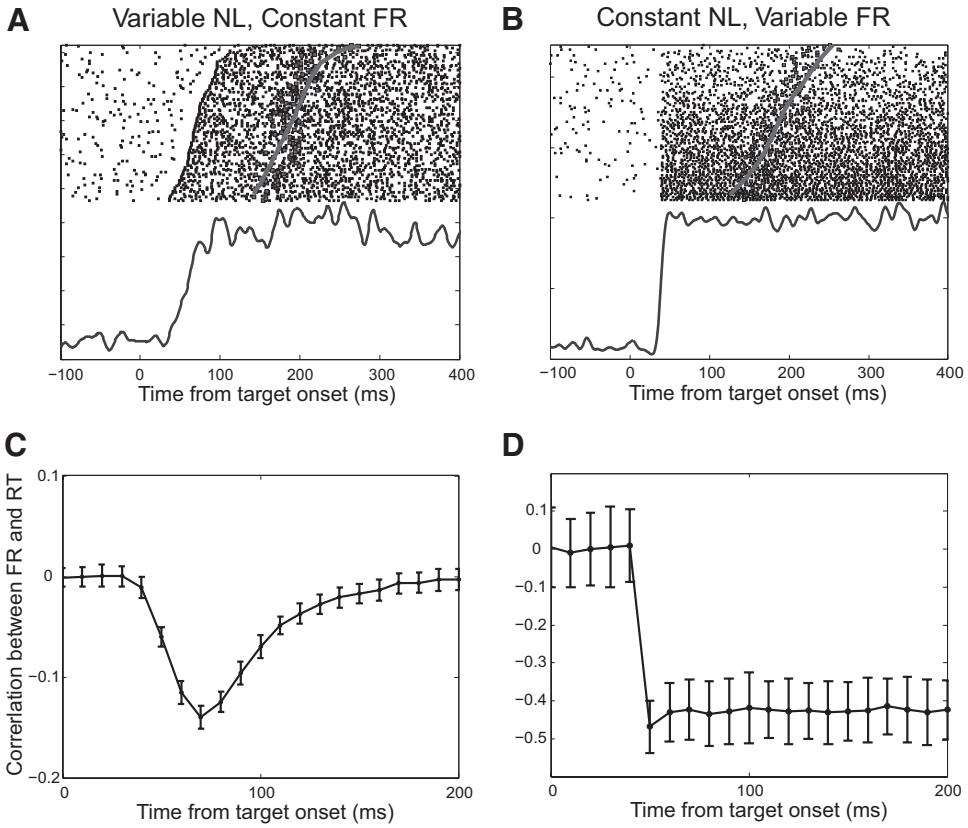

FIG. 10. Simulation of correlation between FR and RT. *A*: raster plot (*top*) of 100 spike trains of a constant response FR generated with a variable NL. From generated spike trains, NL was determined for each trial based on the intertrial interval distribution of spikes during baseline periods. Trials are sorted according to NL. Simulated saccadic onset times coupled to NL are marked (gray symbols) along with their spline approximation (a thick gray curve). A spike density function is shown *below*. *B*: raster plot of 100 spike trains with a constant NL and a variable FR, sorted according to FR. Saccadic onset time is coupled to FR. *C* and *D*: time courses of correlation between FR and RT. For each of 100 cells, 100 trials of *A* or *B* were generated. The spike density during poststimulus epochs of nonoverlapping 10 ms were calculated and correlated with RT, and the average correlations across 100 simulated cells for each of epochs of 10 ms are plotted along their SDs. NL and RT distributions of these artificial cells follow Gaussian distributions and Pearson correlation coefficients were computed. In *D*, the correlation was relatively large, because FR variability was exaggerated in *B*. Note that in *C*, although FR of individual trials was constant, a false correlation between FR and RT emerged and the time course of correlation between FR and RT of Fig. 9 was mimicked.

correlation between FR and RT of Fig. 9 was not reproduced (Fig. 10*D*). The exact values of NL and FR used for simulation within physiological ranges of Fig. 3 were not critical for generating the false correlation, and the pattern of time course of the false correlation strongly depended on the magnitude of variability of NL but not on variability of RT (not shown). We only tested the preceding two conditions, but one can come up with other conditions variously combining coupling of NL and FR to RT. It is also possible that to mimic the experimental time course with a constant FR, the correlation between FR and RT dynamically modulate, but in a complex way in cortical areas yet to be identified. The simulation results demonstrate that a simple model based on the variability of NL of V1 activity is sufficient to explain the apparent correlation between FR and RT and its time course.

Relative contribution of NL and FR for RT information

To examine whether the false correlation between FR and RT was indeed produced by correlation between NL and RT, we compared NL and FR for predicting power of RT in two ways, multiple linear regression and partial correlation analyses, and results from both analyses indicated that FR carried virtually no explanatory power. For these analyses, we used as a measure of FR the mean spike density during the poststimulus time period of 40–130 ms in which the correlation between FR and RT was significant (Fig. 9). First, relative contributions of NL and FR for RT were estimated for each neuron with the following multiple linear regression model, $RT = \alpha + \beta_1 * \text{contrast} + \beta_2 * FR + \beta_3 * NL + \varepsilon$. Note that, in this model, the β coefficients represent unique effects of each predictor in changing RT when all the other predictors in the model are held fixed (Abdi 2003). We used normalized values of neural response and RT (z-scores) to compute the regression coefficients. The mean coefficient for NL term was significantly different from zero, whereas that for FR term was near zero. Calculating FR over different periods (0–100 ms of poststimulus time, target onset to saccade onset) or determination of NL with Poisson spike train analysis resulted in similar results; the mean coefficient for NL term ranged from 0.15 to 0.16 and was statistically significant in all cases, whereas that for FR ranged from −0.02 to 0.01 and was statistically nonsignificant. These results indicate that the false correlation between FR and RT with respect to target onset was indeed caused by correlation between NL and RT and that FR carried no explanatory power for RT. We also estimated the independent contribution of NL and FR for RT with partial correlation analysis. The mean partial correlation coefficient between NL and RT controlling FR calculated over the poststimulus time of 40–130 ms across all contrasts was 0.16 ± 0.19 (1-sample t-test, $P < 0.01$), whereas that between FR and RT controlling NL was 0.01 ± 0.20 (1-sample t-test, $P = 0.21$), indicating again that FR, after removing contributions from NL, contributed little to RT variability and that the correlation between FR and RT of Fig. 9 was a by-product of the correlation between NL and RT.

The explanatory power of the neural response (both NL and FR) for RT was calculated by subtracting R^2 of the model including only contrast variables ($RT = \alpha + \beta_1 * \text{contrast} + \varepsilon$) from R^2 of the full model described in the preceding text. The mean residual R^2 (representing the unique contribution of V1 neural responses) was 0.045, indicating that one V1 neuron explains, on average, ~5% of RT variability. When the output of V1 neurons was pooled using a Monte Carlo simulation, the

partial correlation coefficient between NL and RT increased with the number of pooled neurons; when about 20 V1 cells were pooled, the coefficient increased up to ~0.42 (Fig. 11).

The coefficients reported here are likely to underestimate the true correlation between V1 activity and RT to the extent that there is dependency among individual neurons because pooling activity with repeated sampling inevitably increases the interdependency of data. Also note that all the V1 cells in our sample were used for this simulation, regardless of the magnitude of correlation with RT, and the overall mean correlations are rather low. Correlation between individual cell activity and behavioral response has been reported to be low in detection compared with discrimination task (Britten et al. 1992; Cook and Maunsell 2002).

Possible contribution of internal state

We considered the possibility that slow processes of the animal's internal state, such as attentional or motivational level contributed to the correlation between V1 activity and RT. The slow processes are known to be associated with varying firing patterns of cortical neurons (Bach and Kruger 1986; Evarts 1964; Steriade et al. 1993) and saccadic latency (Groner and Groner 1989). To examine whether slow processes played a role in varying neural activity and RT, we calculated trial auto-covariance (Bair et al. 2001) of NL, FR50, RT, and spontaneous activity. For this, we used z-scores normalized within each stimulus contrast condition of each cell. For example, $FR_n(i)$ is a z-score of FR50 during ith valid trial for the contrast condition n. The trial auto-covariance of $FR_n(i)$, $C(\tau)$, was defined as

$$C(\tau) = \frac{1}{N}\sum_{n=1}^{N}\sum_{i=1}^{T} FR_n(i)FR_n(i+\tau)$$

If neural activity or RT is modulated by internal states with a slow dynamic, correlation coefficients between nearby trials would be significantly higher than zero. We sorted trials within each contrast condition in which two targets were used (n = 182 contrast conditions from 65 neurons having >50 trials) and ordered trials according to chronological order. RT, NL, FR50, and spontaneous activity (mean spike density during prestimulus interval of −200–0 ms) were standardized with z-values within each contrast condition. The coefficients of autocorrelation of these parameters were computed for each condition, and averaged across all conditions. The resulting coefficients indicate the magnitude of response correlation between nearby trials. One-sample t-test at each trial lag revealed that significant correlation ($P < 0.05$) was found for spontaneous activity level between trials with lags up to seven, and little correlation was found between nearby trials in RT, NL, and FR50 (Fig. S2). The lack of correlation of RT between nearby trials suggests that our data were obtained in fairly similar arousal or motivational states. It is unlikely that slow processes, by having a common effect on both V1 activity and RT, modulate the covariation between them. For example, the mean spike density measured over the period from −200 to 0 ms from target onset for the earlier and later RT groups described in the preceding text were not significantly different (−0.07 ± 3.18, one-sample t-test, $P = 0.71$). We conclude that the correlation between NL and RT was not produced by slow changes in the internal state of the animals. Of course, this analysis does not preclude the possible contribution by high-frequency processes that operate within a single trial for correlation between NL and RT.

Laminar evolvement of RT signal in V1

Inputs and outputs of V1 are segregated in a laminar fashion, and neural response properties vary with laminar position (Gilbert 1977; Martinez et al. 2005). To test whether such laminar specialization exists in terms of correlation with RT, we estimated depths of recorded units in reference to the point at which the first visual driving was noted. We emphasize, however, that this is only a crude estimate involving considerable error due to tissue drag as the electrode penetrates the cortical surface despite our efforts to reduce the error by thinning the dura before each recording session.

The cortical layers associated with high spontaneous activity (layers 4A, 4Cα, 4Cβ, and 6) are known to interdigitate with

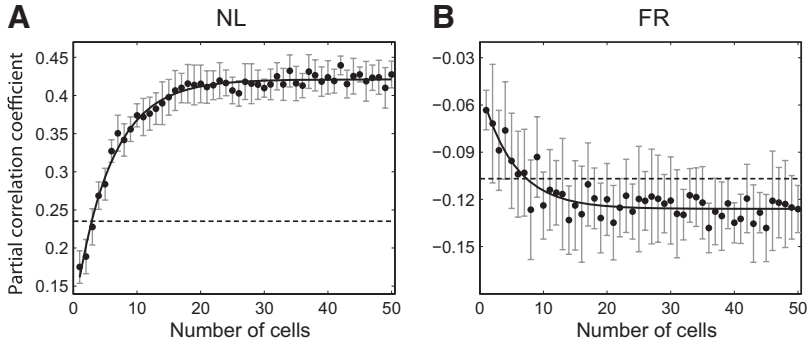

FIG. 11. Correlation between population activity and RT as a function of the size of neural population. *A*: Spearman partial correlation between NL and RT controlling stimulus contrast. *B*: Spearman partial correlation between mean FR and RT controlling stimulus contrast. In both *A* and *B*, each point is the mean and its standard error of 66 random combinations (without replacement) of varying number of single cells from our data set. Solid curves are exponential fits for mean of partial correlations obtained for varying number of cells ranging from 1 to 50 cells, $y = 0.42 - (0.42 - 0.11)\cdot e^{0.18x}$ (*A*) and $y = -0.13 - (-0.13 + 0.05)\cdot e^{-0.19x}$ (*B*). Dashed horizontal lines are the mean values of partial correlation of single neurons from our original data set, 0.23 for NL (*A*) and −0.11 for FR (*B*). The asymptotic value for exponential fit for NL, when neural latency was determined with Poisson spike train analysis, was also 0.42. The asymptotic value for the FR was −0.13. The partial correlation coefficient estimated by single cells ($n = 1$) is smaller than that of experimental data (dashed line). This was caused by setting 3 ms as the class interval of RT required for simulation, whereas actual RT was used for calculating correlation coefficient of experimental data. Setting 1 ms instead of 3 ms as the class interval produced a correlation at $n = 1$ comparable to experimental value for both NL and FR, but slightly delayed saturation of correlation because it inevitably increased the failure in finding experimental trials with RT that matched the randomly chosen RT for simulation.

layers of low spontaneous activity (layers 2/3, 4B, 4Cm, and 5) (Gur et al. 2005). During electrode penetration, we often noted the depths associated with the start or end of high spontaneous activity. However, we feel that these observations were not sufficient to unequivocally discriminate cortical layers because we typically collected data without penetrating all the layers; this would have been required to verify all the alternations in the level of spontaneous activity. Therefore based on the depth of recording site, the FF (variance/mean ratio) of the spike count, and a previous report that related spontaneous activity to V1 laminar position in the awake monkey (Snodderly and Gur 1995), the sample was classified into three depth groups, each spanning 500 μm (Fig. 12). The zero depth of Fig. 12, taken from the depth of the first encounter of neural activity observable via the audio monitor, corresponds to the top of layer 2, and the "superficial" depth group (depth: 0–500 μm) corresponds to layers 2/3 (depth: 200–700 μm of Figs. 3 and 4 of Snodderly and Gur 1995). This group showed a medium-to-high level of spontaneous activity (20.14 $\pm$ 1.71 spike/s) and a medium-to-high FF (1.10 $\pm$ 0.04). The "middle" depth group (depth: 500–1,000 μm) roughly corresponds to layer 4 (Figs. 3 and 4 of Snodderly and Gur 1995) and shows medium spontaneous activity (16.89 $\pm$ 3.64 spike/s) and low FF (0.64 $\pm$ 0.04). The "deep" depth group (1,000–1,500 μm) corresponds to layers 5/6 and possibly the lower tier of layer 4 and shows the lowest baseline activity (14.88 $\pm$ 2.73 spike/s) and medium FF (0.86 $\pm$ 0.05). A division at 1,100 μm between middle and deep depth groups, resulting in the middle depth group spanning 600 μm (500–1,100 μm) and matching layer 4 of Snodderly and Gur (1995) did not influence the results.

The higher overall baseline activity compared with that of Snodderly and Gur (1995) might be due to occasional failure of cell isolation despite every effort to isolate single cells. If the activity at some sites was from multiple units, this would have led to overestimation of correlation as pooling multiple neurons increases correlation (Fig. 11). The mean NL of the middle group across all contrast conditions was 1.6–2.9 ms shorter than the superficial and deep depth groups. These results are consistent with previous studies in terms of the order of synaptic activity in which excitatory synaptic activity first starts in layer 4 and then spreads to superficial and deep layers (Maunsell and Gibson 1992; Mitzdorf and Singer 1978). The FF of the middle group was significantly lower than both superficial and deep depth groups (Mann-Whitney U test, $P < 0.01$ in both comparisons), consistent with the idea that spike variability increases at each processing stage (Kara et al. 2000). These results indirectly support our designation of depth groups.

There was a clear difference in both contrast sensitivity (activity increase per log-unit increase of stimulus contrast) and partial correlations between NL and RT controlling stimulus contrast across depth groups. Most notably, in comparison with the superficial depth group, the deep depth group showed higher partial correlations (Fig. 12*C*) and lower contrast sensitivity (*D*). The mean partial correlation differed significantly between superficial and deep depth groups (Mann-Whitney U test, $P < 0.05$). Contrast sensitivity showed a different pattern; it varied across depth groups being high in the superficial and low in the other groups (Mann-Whitney U test, $P < 0.01$). These results suggest that within V1, RT-related signals evolve from sensory responses following the interlaminar pathways from supragranular to infragranular layers as revealed by anatomical studies (Callaway 1998; Gilbert 1983): i.e., the superficial group reflecting stimulus properties and the deep group reflecting additionally response-related signals.

DISCUSSION

A series of processing is thought to mediate visually guided saccades (e.g., Carpenter et al. 2009): detection of target, perceptual decision as to whether the target is present, and initiation of behavioral response. The RT variability for easily

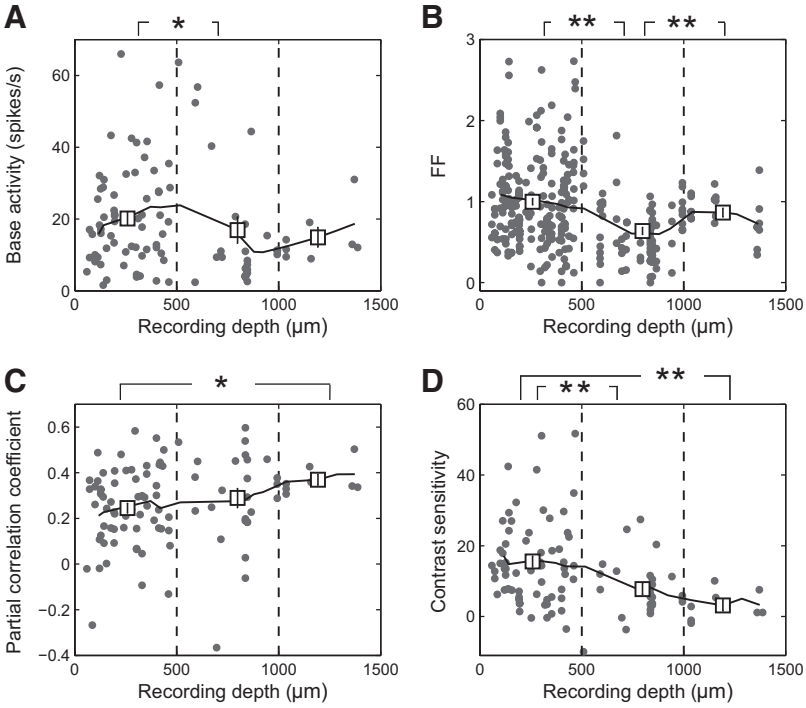

FIG. 12. Relationship between cortical depth and response properties for each of 98 cells for which recording depth was noted. *A*: spontaneous FR during a prestimulus period of 200 ms for each cell. *B*: Fano factor of spike count during the period of 50 ms after NL of each stimulus contrast condition. *C*: Spearman partial correlation coefficient between NL and RT for each cell. *D*: contrast sensitivity of FR50 for each cell. In each panel, the borders between three depth groups (dotted lines) are 500 and 1,000 μm. There were 63, 27, and 8 cells in the superficial, middle, and deep depth groups, respectively. Lines indicate moving average at every 100 μm, and squares and bars represent mean $\pm$ SE for 3 depth groups. Note that depth was read from the microdrive, i.e., the distance the electrode advanced, and thus potentially contains a considerable error in terms of actual depth of cells with respect to cortical surface. Significant differences between depth groups (Mann-Whitney U test) are indicated (asterisk, $P < 0.05$; double asterisk, $P < 0.01$).

detected targets has been attributed to the decision stage (Carpenter and Williams 1995; Smith and Ratcliff 2004), and accordingly neural mechanisms for RT variability have been sought beyond V1, such as the frontal eye field (Hanes and Schall 1996). A major finding of the current study is the covariation between trial-to-trial variability of V1 activity and RT, and we discuss related issues in the following text.

NL versus FR

Previous studies suggested that the information conveyed by NL and FR in V1 is not identical; stimulus contrast is related more to NL than to FR (Gawne et al. 1996b; Reich et al. 2001b). The results obtained in the current study indicate that whereas NL was significantly correlated with RT (Fig. 6), FR was not (Fig. 8). The lack of power of FR in explaining RT variability was unanticipated because FR has been the most frequently used parameter for evaluating the relationship between neural responses and saccadic latency (Roitman and Shadlen 2002; Schall 1991) or behavioral performance (Britten et al. 1996; Nienborg and Cumming 2006; Palmer et al. 2007). However, this might be consistent with potential advantages of spike timing, especially in rapid processing tasks (Thorpe et al. 2001). It has been suggested that a neural code based on the first spike time can be a mechanism for rapid transmission of a visual scene (Gollisch and Meister 2008). The task used in the current study required rapid perceptual judgment because the reward was contingent on correct saccades made within 600 ms of stimulus onset. Under this condition, the integration of V1 output by downstream decision stages focused on spikes within a narrow time period. One can expect that other experimental conditions in which information is integrated over an extended period before initiating a saccade may reveal a stronger correlation between FR and RT. In support of this, most studies reporting relationship between neural response and RT have used tasks in which the RT was larger: 409~795 ms in coherent motion task (Roitman and Shadlen 2002), 250~400 ms in dot-separation task (Ratcliff et al. 2003) or 257~332 ms in figure-ground detection (Super and Lamme 2007; Super et al. 2003a,b). Lowering stimulus contrast in a detection task delays RT (Fig. 3) but appears to be not enough to reveal roles of FR in predicting RT (Fig. 8).

A solution to poor performance of the rate code in a rapid processing condition is to monitor the output of a large number of units (Gautrais and Thorpe 1998). However, the negligible improvement of correlation between FR and RT (Fig. 11*B*) suggests that the rate code is not employed for extracting RT-related signals. On the other hand, the increase in correlation between NL and RT (Fig. 11*A*) suggests that NL is indeed employed because as previously shown in the retina, variation in the first spike time across a neural population will improve performance when the first spike time of the neural population was considered (Gollisch and Meister 2008). The pattern of increase in behavior-related information by pooling neural populations in the present study was remarkably similar to that of Ghose and Harrison (2009), taking into account the difference in analysis method, notably the fact that we used all the neurons recorded, whereas Ghose and Harrison (2009) used the 20 most informative neurons to derive population estimates.

When action potentials were counted with respect to target onset and related to RT, a false correlation between FR and RT emerged (Fig. 9); false because the FR of a neuron itself is not related to RT (Fig. 8). Nevertheless the time course of this correlation reflects a correlation between V1 activity and RT with respect to target onset. The peak correlation occurred at near NL not at the peak FR, again indicating that NL and RT were correlated. The time course of the correlation between V1 activity and RT with respect to target onset is remarkably similar to the impulse response of visual system for saccadic decision (Ludwig et al. 2005). Ludwig et al. (2005) showed that in a rapid perceptual decision task, saccadic decisions were mostly driven by the sensory information during the epoch of 25–75 ms after stimulus onset. The magnitude of correlation between V1 activity and RT with respect to target onset grew rapidly after stimulus onset and decayed thereafter (Fig. 9) and also could be fit with a log-Gaussian function of the following form, $y = -0.08 \cdot e^{-0.5\{[\ln(t/63.98)]^2/(0.64^2)\}}$, where t is time in milliseconds, indicating that the function peaked at 63.98 ms with a scale parameter (0.64). The location of peak correlation is ~64 ms for V1 activity but 35 ms for the psychophysically determined impulse response [using the averages of location and scale parameters from Table 1 of Ludwig et al. (2005) for fitting regression weights] with a difference of 29 ms that probably reflects a transmission delay. Thus the results obtained in the current study support their hypothesis that a "single-shot" output of an early temporal filter providing signals for saccadic decisions resides within V1. The results are also consistent with the observation that spike activity at a fixed delay from stimulus onset was maximally informative about behavioral choice for a rapid perceptual judgment, and thus the reliable correlation between neuronal activity and behavioral choice does not require integration over an extensive period (Chen et al. 2008; Ghose and Harrison 2009). The results from the current study suggest that the origin of the pattern of impulse response, i.e., the peak correlation between neural activity within a brief period after stimulus onset and saccadic decision, is likely to be the variability of NL around which the strongest correlation with perceptual decision occurs.

Nature of relationship between V1 activity and RT

Does V1 activity determine saccadic decisions? Although V1 activity chronologically precedes the saccadic response, and electrical stimulation of V1 evokes a saccadic eye movement in a trained monkey toward the receptive field location of stimulated neurons (Tehovnik et al. 2002), the presence of activity in V1 appears to be neither a sufficient nor necessary condition for saccadic initiation in spatial register as can be seen in a visually guided antisaccade task in which a saccadic eye movement is required in the direction opposite to visual stimulus (Munoz and Everling 2004). The information supplied by V1 output is used according to behavioral requirements, and thus V1 activity is not causally linked to saccadic initiation. On the other hand, both temporal and spatial information on which a successful saccade critically depends can be extracted from the V1 output at least partly. Under conditions in which behavioral requirements remain constant throughout the experiment, as in the current study, V1 activity in a spatial map can provide "when" and "where" signals for saccadic initiation: when signals from the population NL and where

signals from the location of active neurons within a retinotopic map. In this condition, RT depends on V1 activity.

The correlation between V1 activity and RT could arise from a common input that modulates in parallel the excitability of V1 and other structures downstream to V1 that are responsible for saccadic initiation, such as the superior colliculus, thus producing spurious correlations between them. A potential source of the variability of neural activity and the correlation between neural activity and RT could be the cortical state at the time of stimulus presentation (Arieli et al. 1996). The result that NL, but not the mean spike density during the prestimulus period of 200 ms, was significantly different for the early and late RT groups suggests that the magnitude of on-going activity was not the common source resulting in correlation between NL and RT. The lack of correlation in NL and in RT between nearby trials also discounts the possibility that slow processes modulate both NL and RT and produce a spurious correlation between them, although they cause a correlation in spontaneous activity between nearby trials (Fig. S2). Another potential source of variability of V1 activity could be coherent fluctuations in membrane potential preceding the onset of a stimulus in the gamma (20–70 Hz) frequency range (Azouz and Gray 1999). Prestimulus alpha and gamma power in MT was reported to be positively correlated with RT in discriminating perceptual rotation (Wang et al. 2007). To examine whether NL variability of V1 and thus correlation between NL and RT depends on on-going oscillation of cortical activity at the time of target presentation, we analyzed the power of rhythmic discharge of multiunit activity (MUA) during the interval from 500 ms before to 10 ms after the target onset and related this to the NL of single neurons recorded on the same electrode or to RT. We failed to find significant correlations between the power of on-going alpha or gamma-band rhythmic discharge and NL, RT, or FR50 (Fig. S3). Based on these results, we tentatively conclude that on-going oscillatory discharge was not a common source resulting in correlation between NL and RT. Further studies on local field potentials that appear to be more sensitive than spiking activity for detecting behavioral modulation of oscillatory synchronization (Womelsdorf et al. 2006) may help resolve this issue in V1. A significant correlation between NL and RT, but not between FR50 and RT, as well as the differential RT correlation among depth groups, also argues against a common cause for the observed correlation between NL and RT. The variability of V1 activity may also be caused by eye fixation variability (Gur and Snodderly 2006; Gur et al. 1997). However, it is hardly conceivable that the variability in eye position during target presentation produces a significant correlation between NL and RT because saccadic response is also contributed by adjacent cells other than the one under study that may change their responses to the visual target in a manner different from the one under study.

Previous studies have established direct links between neuronal activity and perceptual decisions (Britten et al. 1996; Dodd et al. 2001; Nienborg and Cumming 2006; Palmer et al. 2007; Roitman and Shadlen 2002). The relationship between neural activity along the visual pathway and the latency of visually guided movements has also been studied (Cook and Maunsell 2002; DiCarlo and Maunsell 2005; Super et al. 2003a). Using a figure-ground detection task, Super et al. (2003) reported a strong modulation of V1 neural response for shorter RT but not for longer RT. V1 receives abundant feedback inputs from higher cortical areas as well as feedforward input transmitting sensory information from the retina (Lamme and Roelfsema 2000). The figure-ground contextual modulation started around 130 ms after stimulus onset, suggesting that the modulation depends on feedback from higher areas. In the current study, trial-to-trial variability of NL was correlated with RT, whereas that of FR was not, suggesting that saccadic initiation in our task was primarily driven by the feedforward connection.

ACKNOWLEDGMENTS

We are grateful to Drs. Joseph Malpleli and Daeyeol Lee for helpful comments on the manuscript. We are also very grateful to the reviewers for helpful comments and suggestions. We also thank Drs. Fumiaki Cho and Byung-Hwa Hyun at The Korean National Primate Research Center for help with establishing animal facility, K.-H. Lee for animal care and preparation, Dr. Jee Ho Chang for ocular examination of animals, and N.-E. Kwon for secretarial assistance.

Present addresses: J. Lee, Center for Cognitive Neuroscience at Duke University; H. R. Kim, Department of Brain and Cognitive Sciences at University of Rochester.

GRANTS

This research was supported by the Cognitive Neuroscience Research Program, Brain Frontier Research Program and the Korea Research Foundation Grant 2004-041-H00045 of the Ministry of Korean Education, Science, and Technology.

DISCLOSURES

No conflicts of interest, financial or otherwise, are declared by the author(s).

REFERENCES

Abdi H. Partial regression coefficients. In: *Encyclopedia for Research Methods for the Social Sciences*, edited by Lewis-Beck MS, Bryman A, Liao TF. London: Sage, 2003, p. 978–982.

Albrecht DG, Hamilton DB. Striate cortex of monkey and cat: contrast response function. *J Neurophysiol* 48: 217–237, 1982.

Arieli A, Sterkin A, Grinvald A, Aertsen A. Dynamics of ongoing activity: explanation of the large variability in evoked cortical responses. *Science* 273: 1868–1871, 1996.

Azouz R, Gray CM. Cellular mechanisms contributing to response variability of cortical neurons in vivo. *J Neurosci* 19: 2209–2223, 1999.

Bach M, Kruger J. Correlated neuronal variability in monkey visual cortex revealed by a multi-microelectrode. *Exp Brain Res Expe Hirnforsch* 61: 451–456, 1986.

Bair W, Zohary E, Newsome WT. Correlated firing in macaque visual area MT: time scales and relationship to behavior. *J Neurosci* 21: 1676–1697, 2001.

Box GEP, Jenkins GM, Reinsel GC. *Time Series Analysis: Forecasting and Control.* Englewood Cliffs, NJ: Prentice Hall, 1994.

Brainard DH. The Psychophysics Toolbox. *Spat Vision* 10: 433–436, 1997.

Britten KH, Newsome WT, Shadlen MN, Celebrini S, Movshon JA. A relationship between behavioral choice and the visual responses of neurons in macaque MT. *Visual Neurosci* 13: 87–100, 1996.

Britten KH, Shadlen MN, Newsome WT, Movshon JA. The analysis of visual motion: a comparison of neuronal and psychophysical performance. *J Neurosci* 12: 4745–4765, 1992.

Callaway EM. Local circuits in primary visual cortex of the macaque monkey. *Annu Rev Neurosci* 21: 47–74, 1998.

Carandini M. Amplification of trial-to-trial response variability by neurons in visual cortex. *PLoS Biol* 2: E264, 2004.

Carpenter RH. Contrast, probability, and saccadic latency; evidence for independence of detection and decision. *Curr Biol* 14: 1576–1580, 2004.

Carpenter RH, Reddi BA, Anderson AJ. A simple two stage model predicts response time distributions. *J Physiol* 587: 4051–4062, 2009.

Carpenter RH, Williams ML. Neural computation of log likelihood in control of saccadic eye movements. *Nature* 377: 59–62, 1995.

Chen Y, Geisler WS, Seidemann E. Optimal temporal decoding of neural population responses in a reaction-time visual detection task. *J Neurophysiol* 99: 1366–1379, 2008.

Cook EP, Maunsell JH. Dynamics of neuronal responses in macaque MT and VIP during motion detection. *Nat Neurosci* 5: 985–994, 2002.

DiCarlo JJ, Maunsell JH. Using neuronal latency to determine sensory-motor processing pathways in reaction time tasks. *J Neurophysiol* 93: 2974–2986, 2005.

Dodd JV, Krug K, Cumming BG, Parker AJ. Perceptually bistable three-dimensional figures evoke high choice probabilities in cortical area MT. *J Neurosci* 21: 4809–4821, 2001.

Evarts EV. Temporal patterns of discharge of pyramidal tract neurons during sleep and waking in the monkey. *J Neurophysiol* 27: 152–171, 1964.

Fellous JM, Tiesinga PHE, Thomas PJ, Sejnowski TJ. Discovering spike patterns in neuronal responses. *J Neurosci* 24: 2989–3001, 2004.

Gautrais J, Thorpe S. Rate coding versus temporal order coding: a theoretical approach. *Bio Systems* 48: 57–65, 1998.

Gawne TJ, Kjaer TW, Hertz JA, Richmond BJ. Adjacent visual cortical complex cells share about 20% of their stimulus-related information. *Cereb Cortex* 6: 482–489, 1996a.

Gawne TJ, Kjaer TW, Richmond BJ. Latency: another potential code for feature binding in striate cortex. *J Neurophysiol* 76: 1356–1360, 1996b.

Gawne TJ, Richmond BJ. How independent are the messages carried by adjacent inferior temporal cortical neurons? *J Neurosci* 13: 2758–2771, 1993.

Ghose GM, Harrison IT. Temporal precision of neuronal information in a rapid perceptual judgment. *J Neurophysiol* 101: 1480–1493, 2009.

Gilbert CD. Laminar differences in receptive field properties of cells in cat primary visual cortex. *J Physiol* 268: 391–421, 1977.

Gilbert CD. Microcircuitry of the visual cortex. *Annu Rev Neurosci* 6: 217–247, 1983.

Gollisch T, Meister M. Rapid neural coding in the retina with relative spike latencies. *Science* 319: 1108–1111, 2008.

Groner R, Groner MT. Attention and eye movement control: an overview. *Eur Arch Psychiatry Neurol Sci* 239: 9–16, 1989.

Gur M, Beylin A, Snodderly DM. Response variability of neurons in primary visual cortex (V1) of alert monkeys. *J Neurosci* 17: 2914–2920, 1997.

Gur M, Kagan I, Snodderly DM. Orientation and direction selectivity of neurons in V1 of alert monkeys: functional relationships and laminar distributions. *Cereb Cortex* 15: 1207–1221, 2005.

Gur M, Snodderly DM. High response reliability of neurons in primary visual cortex (V1) of alert, trained monkeys. *Cereb Cortex* 16: 888–895, 2006.

Hanes DP, Schall JD. Neural control of voluntary movement initiation. *Science* 274: 427–430, 1996.

Hanes DP, Thompson KG, Schall JD. Relationship of presaccadic activity in frontal eye field and supplementary eye field to saccade initiation in macaque: Poisson spike train analysis. *Exp Brain Res Exp Hirnforsch* 103: 85–96, 1995.

Henrie JA, Shapley R. LFP power spectra in V1 cortex: the graded effect of stimulus contrast. *J Neurophysiol* 94: 479–490, 2005.

Jones JP, Palmer LA. The two-dimensional spatial structure of simple receptive fields in cat striate cortex. *J Neurophysiol* 58: 1187–1211, 1987.

Judge SJ, Richmond BJ, Chu FC. Implantation of magnetic search coils for measurement of eye position: an improved method. *Vision Res* 20: 535–538, 1980.

Kara P, Reinagel P, Reid RC. Low response variability in simultaneously recorded retinal, thalamic, and cortical neurons. *Neuron* 27: 635–646, 2000.

Kenet T, Bibitchkov D, Tsodyks M, Grinvald A, Arieli A. Spontaneously emerging cortical representations of visual attributes. *Nature* 425: 954–956, 2003.

Kohn A, Smith MA. Stimulus dependence of neuronal correlation in primary visual cortex of the macaque. *J Neurosci* 25: 3661–3673, 2005.

Kveraga K, Boucher L, Hughes HC. Saccades operate in violation of Hick's law. *Exp Brain Res Exp Hirnforsch* 146: 307–314, 2002.

Lamme VA, Roelfsema PR. The distinct modes of vision offered by feedforward and recurrent processing. *Trends Neurosci* 23: 571–579, 2000.

Lawrence BM, St John A, Abrams RA, Snyder LH. An anti-Hick's effect in monkey and human saccade reaction times. *J Vision* 8: 26 21571–27, 2008.

Lee D, Port NL, Kruse W, Georgopoulos AP. Variability and correlated noise in the discharge of neurons in motor and parietal areas of the primate cortex. *J Neurosci* 18: 1161–1170, 1998.

Legendy CR, Salcman M. Bursts and recurrences of bursts in the spike trains of spontaneously active striate cortex neurons. *J Neurophysiol* 53: 926–939, 1985.

Lewicki MS. A review of methods for spike sorting: the detection and classification of neural action potentials. *Network* 9: R53–78, 1998.

Ludwig CJ, Gilchrist ID, McSorley E, Baddeley RJ. The temporal impulse response underlying saccadic decisions. *J Neurosci* 25: 9907–9912, 2005.

Mainen ZF, Sejnowski TJ. Reliability of spike timing in neocortical neurons. *Science* 268: 1503–1506, 1995.

Martinez LM, Wang Q, Reid RC, Pillai C, Alonso JM, Sommer FT, Hirsch JA. Receptive field structure varies with layer in the primary visual cortex. *Nat Neurosci* 8: 372–379, 2005.

Maunsell JH, Gibson JR. Visual response latencies in striate cortex of the macaque monkey. *J Neurophysiol* 68: 1332–1344, 1992.

Mitzdorf U, Singer W. Prominent excitatory pathways in the cat visual cortex (A 17 and A 18): a current source density analysis of electrically evoked potentials. *Exp Brain Res Exp Hirnforsch* 33: 371–394, 1978.

Munoz DP, Everling S. Look away: the anti-saccade task and the voluntary control of eye movement. *Nat Rev* 5: 218–228, 2004.

Nauhaus I, Busse L, Carandini M, Ringach DL. Stimulus contrast modulates functional connectivity in visual cortex. *Nat Neurosci* 12: 70–76, 2009.

Nienborg H, Cumming BG. Macaque V2 neurons, but not V1 neurons, show choice-related activity. *J Neurosci* 26: 9567–9578, 2006.

Osborne LC, Lisberger SG, Bialek W. A sensory source for motor variation. *Nature* 437: 412–416, 2005.

Palmer C, Cheng SY, Seidemann E. Linking neuronal and behavioral performance in a reaction-time visual detection task. *J Neurosci* 27: 8122–8137, 2007.

Pelli DG. The VideoToolbox software for visual psychophysics: transforming numbers into movies. *Spat Vision* 10: 437–442, 1997.

Ratcliff R, Cherian A, Segraves M. A comparison of macaque behavior and superior colliculus neuronal activity to predictions from models of two-choice decisions. *J Neurophysiol* 90: 1392–1407, 2003.

Reich DS, Mechler F, Victor JD. Independent and redundant information in nearby cortical neurons. *Science* 294: 2566–2568, 2001a.

Reich DS, Mechler F, Victor JD. Temporal coding of contrast in primary visual cortex: when, what, and why. *J Neurophysiol* 85: 1039–1050, 2001b.

Richmond BJ, Optican LM, Spitzer H. Temporal encoding of two-dimensional patterns by single units in primate primary visual cortex. I. Stimulus-response relations. *J Neurophysiol* 64: 351–369, 1990.

Roberts MJ, Zinke W, Guo K, Robertson R, McDonald JS, Thiele A. Acetylcholine dynamically controls spatial integration in marmoset primary visual cortex. *J Neurophysiol* 93: 2062–2072, 2005.

Roitman JD, Shadlen MN. Response of neurons in the lateral intraparietal area during a combined visual discrimination reaction time task. *J Neurosci* 22: 9475–9489, 2002.

Sanger TD. Decoding neural spike trains: calculating the probability that a spike train and an external signal are related. *J Neurophysiol* 87: 1659–1663, 2002.

Sceniak MP, Ringach DL, Hawken MJ, Shapley R. Contrast's effect on spatial summation by macaque V1 neurons. *Nat Neurosci* 2: 733–739, 1999.

Schall JD. Neuronal activity related to visually guided saccades in the frontal eye fields of rhesus monkeys: comparison with supplementary eye fields. *J Neurophysiol* 66: 559–579, 1991.

Schall JD, Hanes DP, Thompson KG, King DJ. Saccade target selection in frontal eye field of macaque. I. Visual and premovement activation. *J Neurosci* 15: 6905–6918, 1995.

Schiller PH, Finlay BL, Volman SF. Short-term response variability of monkey striate neurons. *Brain Res* 105: 347–349, 1976.

Schmolesky MT, Wang Y, Hanes DP, Thompson KG, Leutgeb S, Schall JD, Leventhal AG. Signal timing across the macaque visual system. *J Neurophysiol* 79: 3272–3278, 1998.

Schneidman E, Freedman B, Segev I. Ion channel stochasticity may be critical in determining the reliability and precision of spike timing. *Neural Comput* 10: 1679–1703, 1998.

Segraves MA, Park K. The relationship of monkey frontal eye field activity to saccade dynamics. *J Neurophysiol* 69: 1880–1889, 1993.

Shadlen MN, Newsome WT. The variable discharge of cortical neurons: implications for connectivity, computation, and information coding. *J Neurosci* 18: 3870–3896, 1998.

Smith PL, Ratcliff R. Psychology and neurobiology of simple decisions. *Trends Neurosci* 27: 161–168, 2004.

Snodderly DM, Gur M. Organization of striate cortex of alert, trained monkeys (*Macaca fascicularis*): ongoing activity, stimulus selectivity, and widths of receptive field activating regions. *J Neurophysiol* 74: 2100–2125, 1995.

Steriade M, McCormick DA, Sejnowski TJ. Thalamocortical oscillations in the sleeping and aroused brain. *Science* 262: 679–685, 1993.

Super H, Lamme VA. Strength of figure-ground activity in monkey primary visual cortex predicts saccadic reaction time in a delayed detection task. *Cereb Cortex* 17: 1468–1475, 2007.

Super H, Spekreijse H, Lamme VA. Figure-ground activity in primary visual cortex (V1) of the monkey matches the speed of behavioral response. *Neurosci Lett* 344: 75–78, 2003a.

Super H, van der Togt C, Spekreijse H, Lamme VA. Correspondence of presaccadic activity in the monkey primary visual cortex with saccadic eye movements. *Proc Natl Acad Sci USA* 101: 3230–3235, 2004.

Super H, van der Togt C, Spekreijse H, Lamme VA. Internal state of monkey primary visual cortex (V1) predicts figure-ground perception. *J Neurosci* 23: 3407–3414, 2003b.

Tallon-Baudry C, Bertrand O, Henaff MA, Isnard J, Fischer C. Attention modulates gamma-band oscillations differently in the human lateral occipital cortex and fusiform gyrus. *Cereb Cortex* 15: 654–662, 2005.

Tehovnik EJ, Slocum WM, Schiller PH. Differential effects of laminar stimulation of V1 cortex on target selection by macaque monkeys. *Eur J Neurosci* 16: 751–760, 2002.

Thompson KG, Hanes DP, Bichot NP, Schall JD. Perceptual and motor processing stages identified in the activity of macaque frontal eye field neurons during visual search. *J Neurophysiol* 76: 4040–4055, 1996.

Thorpe S, Delorme A, Van Rullen R. Spike-based strategies for rapid processing. *Neural Network* 14: 715–725, 2001.

Tolhurst DJ, Movshon JA, Dean AF. The statistical reliability of signals in single neurons in cat and monkey visual cortex. *Vision Res* 23: 775–785, 1983.

Tsodyks M, Kenet T, Grinvald A, Arieli A. Linking spontaneous activity of single cortical neurons and the underlying functional architecture. *Science* 286: 1943–1946, 1999.

VanRullen R, Koch C. Is perception discrete or continuous? *Trends Cogn Sci* 7: 207–213, 2003.

Vogels R, Spileers W, Orban GA. The response variability of striate cortical neurons in the behaving monkey. *Exp Brain Res ExpHirnforsch* 77: 432–436, 1989.

Wang Z, Maier, A, Logothetis, NK, Leopold DA, Liang H. Prestimulus activity in area MT predicts psychophysical performance in a bistable motion task. *Soc Neurosci Abstr* 716.5, 2007.

Wheeless LL Jr, Boynton RM, Cohen GH. Eye-movement responses to step and pulse-step stimuli. *J Opt Soc Am* 56: 956–960, 1966.

Wiener MC, Richmond BJ. Using response models to estimate channel capacity for neuronal classification of stationary visual stimuli using temporal coding. *J Neurophysiol* 82: 2861–2875, 1999.

Womelsdorf T, Fries P, Mitra PP, Desimone R. Gamma-band synchronization in visual cortex predicts speed of change detection. *Nature* 439: 733–736, 2006.

Xu ZM, Ivanusic JJ, Bourke DW, Butler EG, Horne MK. Automatic detection of bursts in spike trains recorded from the thalamus of a monkey performing wrist movements. *J Neurosci Methods* 91: 123–133, 1999.